

Improving exponential-family random graph models for bipartite networks

Alex Stivala^{1,*}, Peng Wang^{2,1}, and Alessandro Lomi³

¹Institute of Computing, Università della Svizzera italiana, Via Giuseppe Buffi 13, 6900 Lugano, Switzerland

²Centre for Transformative Innovation, Swinburne University of Technology, John Street, Hawthorn VIC 3122, Australia

³Università della Svizzera italiana, Via Giuseppe Buffi 13, 6900 Lugano, Switzerland

*Corresponding author: alexander.stivala@usi.ch

February 5, 2025

Abstract

Bipartite graphs, representing two-mode networks, arise in many research fields. These networks have two disjoint node sets representing distinct entity types, for example persons and groups, with edges representing associations between the two entity types. In bipartite graphs, the smallest possible cycle is a cycle of length four, and hence four-cycles are the smallest structure to model closure in such networks. Exponential-family random graph models (ERGMs) are a widely used model for social, and other, networks, including specifically bipartite networks. Existing ERGM terms to model four-cycles in bipartite networks, however, are relatively rarely used. In this work we demonstrate some problems with these existing terms to model four-cycles, and define new ERGM terms to help overcome these problems. The position of the new terms in the ERGM dependence hierarchy, and their interpretation, is discussed. The new terms are demonstrated in simulation experiments, and their application illustrated with ERGM models of empirical networks ranging in size from hundreds of nodes to hundreds of thousands of nodes.

Keywords— bipartite graph, two-mode network, exponential-family random graph model, ERGM, four-cycle

1 Introduction

Bipartite graphs are graphs whose nodes can be partitioned into two disjoint sets, such that an edge exists only between nodes in different sets. Such graphs have important applications in representing two-mode networks, which are networks in which there are two types of nodes, with edges possible only between nodes of different types. An important example of a two-mode network is an affiliation network, in which one type of node represents a person, the other type of node represents a group, and an edge represents membership of a person in a group [1]. Two-mode networks have applications not only in sociology, but also biology, ecology, political science, psychology, finance, and economics; for a recent review of applications and methods for two-mode networks, see Neal *et al.* [2]. Bipartite networks also arise as representing the meso-level network in the conceptualization and analysis of multilevel networks [3].

Two-mode networks can be studied by means of their projections onto one-mode (unipartite) networks, thereby allowing the use of existing methods for one-mode networks, however this can result in lost information, and properties of the one-mode networks (such as high clustering coefficients) that are due to the projection process rather than the original data [4]. Although the former problem can be overcome by using both projections in analyses [5, 6], it is still desirable to directly study the original two-mode network, for which specific methods are required [4].

In studying one-mode networks, a central concept is triadic closure, the tendency for a path of length two (a “two-path”; three nodes connected by two edges) to be “closed” into a triangle by the addition of a third edge. In the context of a social network, this is the process of a friend of a friend becoming themselves a friend, and is perhaps most well known via the “strength of weak ties” [7] argument, whereby an open two-path of strong ties is the “forbidden triad”, which is “forbidden” because the two actors with strong ties to a common third actor must themselves have a strong tie. In a bipartite network, however, a closed triad (triangle) is impossible; indeed it is a defining feature of bipartite

graphs that only cycles of even length are possible [8]. Therefore, the smallest possible cycle in a bipartite graph is a four-cycle, and hence four-cycles are frequently used to measure closure in bipartite networks [9, 10].

Exponential random graph models (ERGMs) are a widely used model for social [11–14], and other [15–17] networks. Specific forms of the ERGM have been developed for two-mode networks [18–21], however, as we shall show in this work, existing ERGM models for bipartite networks often have problems modelling four-cycles, and hence can frequently not adequately model closure in bipartite networks.

In this work, we will show that, despite the importance of four-cycles in two-mode networks, ERGM terms to model four-cycles in such networks are relatively rarely used, in contrast to the ubiquity of terms modelling triadic closure in one-mode networks. We will then describe some problems with existing configurations for modelling four-cycles that could explain their relatively infrequent use, and propose new ERGM configurations for modelling four-cycles to help overcome these problems. We will discuss the interpretation of these new parameters, and their position in the dependence hierarchy of Pattison & Snijders [22]. We will then demonstrate the new configurations using simulation experiments and apply them in ERGM modelling of seven empirical networks in a variety of domains (ecology, criminology, and sociology) and ranging in size from hundreds of nodes to hundreds of thousands of nodes.

2 The exponential-family random graph model (ERGM)

An ERGM is a probability distribution with the form

$$\Pr_{\theta}(X = x) = \frac{1}{\kappa(\theta)} \exp\left(\sum_C \theta_C g_C(x)\right) \quad (1)$$

where

- $X = [X_{ij}]$ is square binary matrix of random tie variables,
- x is a realization of X ,
- C is a “configuration”, a set of nodes and a subset of ties between them, designed in order to model a particular structure of interest,
- $g_C(x)$ is the network statistic for configuration C ,
- θ is a vector of model parameters, where each θ_C is the parameter corresponding to configuration C ,
- $\kappa(\theta) = \sum_{x \in G_n} \exp(\sum_C \theta_C g_C(x))$, where G_n is the set of all square binary matrices of order n (graphs with n nodes), is the normalising constant to ensure a proper distribution.

We will use the notation x_{ij} (where $1 \leq i \leq n$, $1 \leq j \leq n$) for elements of the binary adjacency matrix x . In this work we consider only the case of undirected networks, so $x_{ij} = x_{ji}$, and the cardinality of G_n is $|G_n| = 2^{n(n-1)/2}$. In the case of bipartite networks, the two disjoint node sets are denoted A and B , with sizes $N_A = |A|$ and $N_B = |B|$ respectively, and so $N_A + N_B = n$, and $x_{ij} = 0$ if both i and j are in node set A or both i and j are in node set B . In this bipartite case, the normalising constant is $\kappa(\theta) = \sum_{x \in G_{N_A, N_B}^{\text{Bipartite}}} \exp(\sum_C \theta_C g_C(x))$, where $G_{N_A, N_B}^{\text{Bipartite}}$ is the set of all bipartite graphs with node set sizes N_A and N_B . This set has cardinality $|G_{N_A, N_B}^{\text{Bipartite}}| = 2^{N_A N_B}$.

Estimating the value of the parameter vector θ which maximises the probability of the observed graph, that is, the maximum likelihood estimator (MLE), enables inferences regarding the under-representation (negative and statistically significant estimate) or over-representation (positive and statistically significant estimate) of the corresponding configurations. These inferences are conditional on the other configurations included in the model, which need not be independent.

Estimating the MLE of (1) is computationally intractable due to the normalising constant $\kappa(\theta)$ (specifically, the size of the set of graphs it sums over). Therefore, Markov chain Monte Carlo (MCMC) methods are usually used [23–25]. One such algorithm is the “Equilibrium Expectation” (EE) algorithm [26–28], which was recently shown to converge to the MLE [17, 28].

ERGM models with only simple configurations (such as the Markov edge plus triangle model) can be prone to problems with phase transitions or “near-degeneracy” [14, 29–35]. Such problems are typically avoided by the use

of “alternating” [30, 36, 37] or “geometrically weighted” [38, 39] configurations. The former are parameterised with a decay parameter λ controlling the rate at which the weight of contributions from additional terms in the statistic decay. The corresponding parameter for the geometrically weighed configurations can be estimated as part of the model, in which case it becomes a “curved ERGM” [40], however in this work we will use fixed values of λ for the “alternating” configurations.

3 Literature survey

In order to get an overview of which effects are used in modelling bipartite networks with ERGMs, and how well they fit four-cycles, we conducted a comprehensive survey of publications which included ERGM models of bipartite networks. To be included, a publication must contain one or more ERGM models of one or more empirical bipartite (two-mode) networks. There must be sufficient detail given to know at least the parameters included in the models, and their estimated signs and statistical significance. Models of one-mode projections of two-mode networks were excluded; we only consider ERGM models of the bipartite network itself. Models of multilevel networks were excluded, although if there is a model of just the cross-level (bipartite) network, this is included.

We used Google Scholar (search date 24 November 2022) to search for papers with terms “bipartite“ and “ergm”, “bpnet” and “ergm”, “statnet” and “bipartite”, and “gwb1dsp” or “gwb2dsp” (the latter being statnet [41, 42] terms used for bipartite networks). We also included papers that we had prior knowledge of being about bipartite ERGMs, and followed backward and forward citations (using Google Scholar for the latter) to find other relevant papers. The papers included in the survey are listed in Table A1 (Appendix A).

Most of the models in Table A1 were estimated with the BpNet [43], MPNet [44, 45] or statnet [41, 42, 46–50] software, but a small number were estimated either by maximum pseudo-likelihood estimation (MPLE) or with Bayesian methods using the Bergm [51, 52] software. The one model included that was estimated with Bergm contains no terms to model four-cycles or goodness-of-fit tests including four-cycles [53]. Of the ten models (across three publications) estimated by MPLE, only one contains a term to model four-cycles, and this is found to be positive and significant [54].

Table 1 summarises the parameter estimates in models from the literature in Table A1 that were estimated using BpNet or MPNet, and contain the four-cycles parameter C_4 , or the bipartite alternating k -two-path parameters ($K-C_P$ and $K-C_A$ in BpNet, XACA and XACB in MPNET) defined in Wang *et al.* [18]. Less than a third (20/63) include the four-cycles parameter, less than half (30/63) include either of the two alternating k -two-path parameters, and less than 30% (17/63) include both $K-C_P$ and $K-C_A$.

Table 1: Counts of parameters in models estimated by BpNet or MPNet (total 63) in the reviewed literature.

	C_4	$K-C_P$	$K-C_A$
Total estimated	20	30	25
Negative	14	20	15
Negative and signif.	5	14	9
Positive	6	10	10
Positive and signif.	4	7	2

Table 2 summarises the parameter estimates in models from the literature in Table A1 that were estimated using statnet, and which contain the four-cycle term, the bipartite geometrically weighted dyadwise shared partner distribution (gwb1dsp or gwb2dsp) term, the statnet equivalent of the $K-C_P$ and $K-C_A$ parameters, or the geometrically weighted non-edgewise shared partner (gwensp) term. The counts for gwb1dsp and gwb2dsp include those for the bipartite geometrically weighted non-edgewise shared partner terms gwb1nsp and gwb2nsp, which are equivalent to gwb1dsp and gwb2dsp, respectively, for bipartite networks. Only one model estimated with statnet contained an explicit term for four-cycles [55]. Further, only 5/43 models contain a gwb1dsp or gwb2dsp term at all, and only two models contain both (Lubell & Robbins [56] have two models, both of which include both gwb1nsp and gwb2nsp).

Less than a quarter (26/117) of the models include an explicit assessment of goodness-of-fit to four-cycles, and of those, the majority (18/26) are good. Only seven of these are for models that explicitly include C_4 as a model parameter, and, as expected of any converged model containing this term, these models fit four-cycles well. Conversely, all of the models which are described as having a poor fit to four-cycles in the goodness-of-fit procedure are models that

Table 2: Counts of parameters in models estimated by statnet (total 43) in the reviewed literature. The counts for `gwb1dsp` and `gwb2dsp` include those for the equivalent parameters `gwb1nsp` and `gwb2nsp`, respectively.

	cycle(4)	gwb1dsp	gwb2dsp	gwnsp
Total estimated	1	2	5	4
Negative	1	1	2	1
Negative and signif.	1	1	0	0
Positive	0	1	3	3
Positive and signif.	0	1	2	3

do not contain the C_4 parameter. However, of these eight models, five contain either $K-C_A$ or $K-C_P$, and one contains both.

This relative rarity of models containing terms to model closure (four-cycles) in bipartite networks, or assess goodness-of-fit to four-cycles, is in stark contrast to ERGM modelling for one-mode networks, where terms modelling triadic closure, such as triangles, alternating- k -triangles, or geometrically weighted edgewise shared partners (`gwersp` in statnet) are almost always included in models, since triadic closure (as evidenced by clustering, or transitivity, in the network), is a well-known feature of social networks [7, 57, 58]. For example, Clark & Handcock [59] use the latent order logistic (LOLOG) model [60] to reproduce ERGM models for 13 networks from peer reviewed papers, and all of these models contain alternating- k -triangles [36, 61–63], `gwersp` [64–69], or three-cycles [61, 70] terms, and in the majority of cases the results are able to be replicated with a triangle term in the LOLOG model [59]. And yet, despite higher than expected numbers of four-cycles (or bipartite clustering coefficient) being a notable feature of some bipartite networks, such as director interlock networks [9, 10], and collaboration and communication networks [10], the literature survey presented here shows that terms to model four-cycles are relatively rarely used in published ERGM models of bipartite networks. This could be due to researchers choosing not to model bipartite closure, however, as shown by some examples in the following section, it can also be due to difficulties in obtaining converged model estimates when using existing model terms.

4 Problems with existing bipartite ERGM statistics

It is notable that in the original paper proposing $K-C_A$ and $K-C_P$ configurations [18], they are explicitly described as k -two-path statistics, and in fact they are just bipartite versions of the one-mode alternating- k -two-path statistic, representing multiple shared partners (`gwdsp` in statnet, and then later `gwb1dsp` and `gwb2dsp` for bipartite networks). There is, however, already some “semantic slippage” into interpreting them as “cycles” or “closure” — even though they only actually include cycles (closure) when $k > 1$ ($k = 1$ is a two-path, $k = 2$ is a four-cycle; see Fig. 3 in Wang *et al.* [18]). For example, “... a better chance of achieving model convergence when closure effects ($K - C_P$ and $K - C_A$) are included in the model.” [18, p. 22]. Even the name $K-C_A$ (or $K-C_P$) suggests “cycle” or “closure” by the use of the “C” (C_4 is used for four-cycles in the paper). Wang *et al.* [19] goes back to naming the $K-C_P$ and $K-C_A$ statistics as A_2P-A and A_2P-B and describing them as “shared affiliations (alternating two-paths)” [19, p. 213]. However the MPNet terminology is $XACA$ and $XACB$ [44, 45], again with the “C” suggestive of cycles or closure, and the EstiNetDirected [71] software (<https://github.com/stivalaa/EstiNetDirected>) refers to these effects as `BipartiteAltKCyclesA` and `BipartiteAltKCyclesB`.

In the influential book edited by Lusher *et al.* [11], Wang [20] describes $K-C_A$ and $K-C_P$ explicitly as “alternating A cycles” and “alternating P cycles” [20, p. 124], with [20, Fig. 10.11] captioned “Alternating 2-paths” but with the figure panels labelled “A cycles (KCA)” and “P cycles (KCP)” respectively [20, p. 125]. This description or interpretation is carried over into the empirical part of the book, with Harrigan & Bond [72], applying bipartite ERGM to a director interlock network, describing $K-C_P$ and $K-C_A$ as “alternating k -cycles” for directors and corporations respectively [72, p. 266], and in the ERGM results tables as “Director 4-cycles” and “Corporation 4-cycles” [72, pp. 268-269]. It is also notable that Harrigan & Bond [72] describes the difficulty of fitting models with $K-C_A$ and $K-C_P$ and the resulting poor goodness-of-fit for the four-cycle statistic:

We found for this particular network that we cannot have both $K-C_P$ and $K-C_A$ in the same model due to convergence issues. In line with Wang, Sharpe, Robins, and Pattison (2009), we present two alternative models, one with each possible k -cycle parameter. ... However, in line with Wang, Sharpe, Robins, and

Pattison (2009), we had a poor fit on the classic 4-cycle parameter [C4], which suggests that improving these structural effects is a substantial area of future research.

[72, p. 267]

Given the results of the literature review described in Section 3 (which includes Harrigan & Bond [72]) it would seem, however, that no such research improving these structural effects has been published yet, and this work may be the first attempt to do so.

We may conclude from this that the $K-C_A$ and $K-C_P$ statistics count too many things other than four-cycles to be usefully used and interpreted as bipartite closure in many cases. Specifically, they count two-paths as their first (highest weighted) term. This results in situations where long paths or cycles contribute to the $K-C_P$ and $K-C_A$ statistics, despite having exactly zero four-cycles (see Table 3). Perhaps even more problematically, high-degree nodes, or stars, for example the “Nine-star” structure in Table 3, result in large values of $K-C_A$ or $K-C_P$ ($XACA$ or $XACB$ in MPNet terminology), depending on which node set the hub node is in, but also have exactly zero four-cycles. It seems clear that large networks are likely to contain many stars, and many paths (of length two or more; and note that a two-star is just a two-path), as well as large cycles [73, 74], and these will contribute to large values of the $K-C_P$ and/or $K-C_A$ statistics, but nothing to the number of four-cycles (the C_4 statistic).

In addition, interpretation of the alternating k -two-paths parameter is problematic: “In this article, we do not concentrate on alternating k -two-path parameters. For some data, we have found it important to include them in models but further work is needed to understand better their effect when included with other parameters” [36, p. 201]. Martin [75] described this as the authors “being somewhat mystified by this statistic” [75, p. 86], and that most ERGM modellers would not be able to describe a “clear behavioral-process analogue to the once-canonical alternating two paths statistic” [75, p. 86].

Therefore, we propose a new statistic that counts four-cycles (and not two-paths), but which is less prone to problems with near-degeneracy than the simple four-cycles parameter. (A simpler new statistic, based on $K-C_A$ and $K-C_P$ but which does not count two-paths, which turns out to be more prone to near-degeneracy than $K-C_A$ and $K-C_P$, is described in Appendix B).

5 New statistics for modelling four-cycles in bipartite ERGMs

Let

$$L_2(i, j) = \sum_{h \neq i, j} x_{ih} x_{hj} \quad (2)$$

be the number of two-paths connecting node i to node j . Since a four-cycle is a combination of two two-paths [30, p. 123], the number of four-cycles is

$$C_4 = \frac{1}{2} \sum_{i < j} \binom{L_2(i, j)}{2}. \quad (3)$$

The sum in equation (3) is over the $\binom{n}{2}$ pairs of nodes in the graph, with the factor of $\frac{1}{2}$ to account for the double-counting due to the symmetry of each four-cycle containing two distinct pairs of nodes, each connected by two two-paths. The number of four-cycles containing a particular node i is

$$C_4(i) = \sum_{j \neq i} \binom{L_2(i, j)}{2} \quad (4)$$

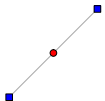
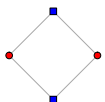
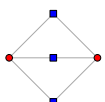
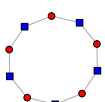
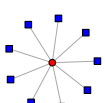
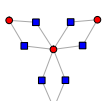
$$= \sum_{\{j: d(i, j)=2\}} \binom{L_2(i, j)}{2} \quad (5)$$

where $d(i, j)$ is the geodesic distance from i to j . Some illustrative examples of the value of $C_4(i)$ for different nodes in some small graphs are shown in Fig. 1.

The total number of four-cycles (3) can also be expressed in terms of the number of four-cycles at each node (4) as

$$C_4 = \frac{1}{4} \sum_i C_4(i) \quad (6)$$

Table 3: Statistics of some example bipartite networks. L is the number of edges, C_4 the number of four-cycles, and $BpNP4CA$ and $BpNP4CB$ are the new statistics $BipartiteFourCyclesNodePowerA$ and $BipartiteFourCyclesNodePowerB$. Nodes in node set A are represented as red circles, and nodes in node set B as blue squares.

Name	Visualization	N_A	N_B	L	C_4	$XACA$	$XACB$	$BpNP4CA$	$BpNP4CB$
Two-path		1	2	2	0	1	0	0	0
Four-cycle		2	2	4	1	1.5	1.5	2	2
Four-cycles-3		2	3	6	3	4.5	1.75	3.4641	4.24264
Ten-cycle		5	5	10	0	5	5	0	0
Nine-star		1	9	9	0	36	0	0	0
Four-fan-3		4	6	12	3	16.5	4.5	4.73205	6

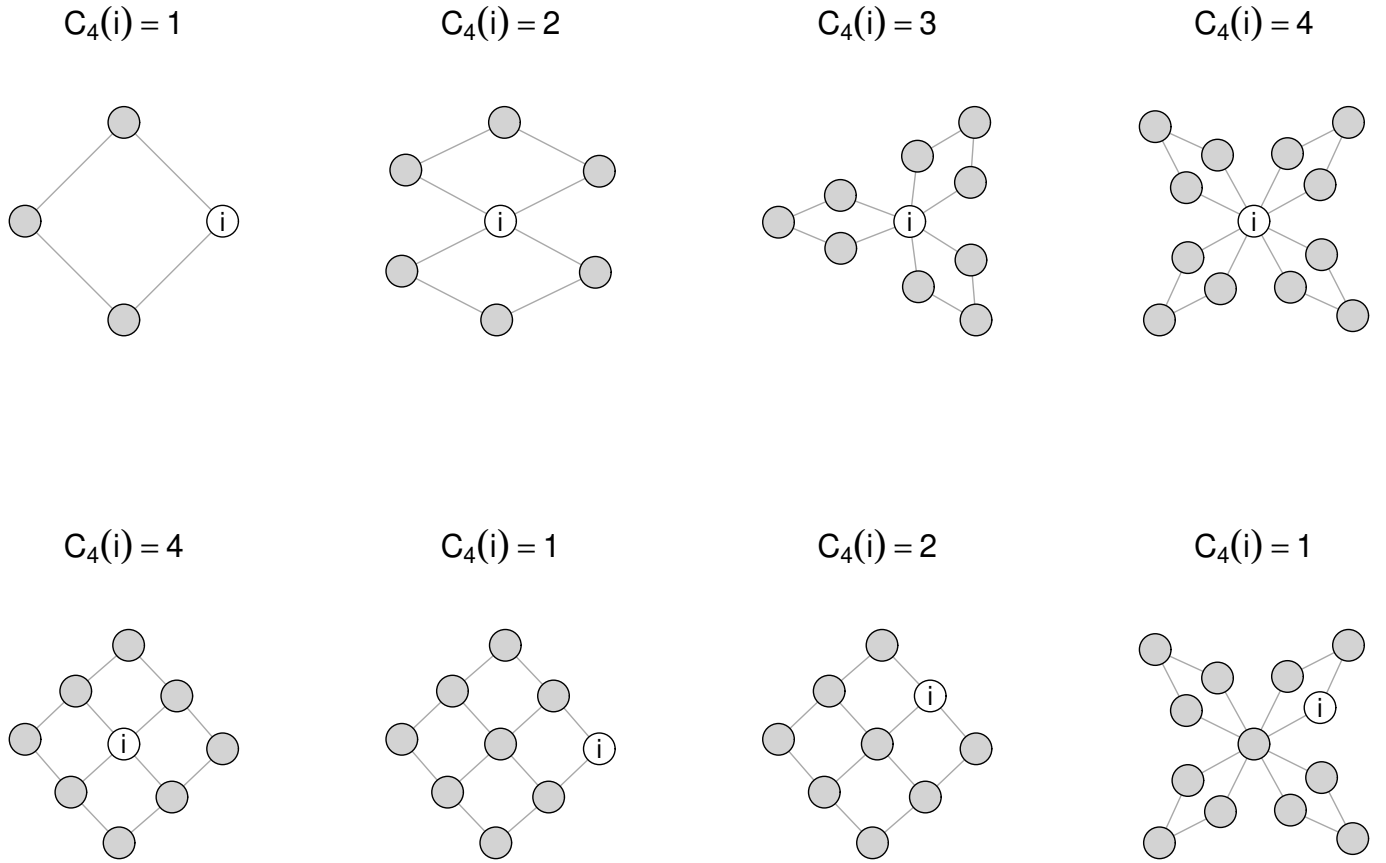


Figure 1: $C_4(i)$ is the number of four-cycles involving a node i .

where the factor of $\frac{1}{4}$ accounts for the fact that each four-cycle is counted four times, once for each node it contains. The FourCyclesNodePower statistic is then defined as

$$z_{\text{FourCyclesNodePower}}(\alpha) = \sum_i [C_4(i)^\alpha] \quad (7)$$

where $0 < \alpha \leq 1$ is the exponent for, in the terminology of Wilson *et al.* [76], the “ α -inside” weighting, since the subgraph counts ($C_4(i)$ here) are exponentiated before summing over all subgraphs. The “ α -outside” weighting would be to exponentiate the statistic after summing over all subgraphs, that is, in this case it would be $[\sum_i C_4(i)]^\alpha$. As discussed in Wilson *et al.* [76], the α -inside weighting leads to local dependence as usually used in ERGMs, while the α -outside weighting leads to global dependence, in which all ties are dependent on each other to some degree [76, p. 41]. The nature of the local dependencies induced by the new change statistics defined here using the α -inside weighting are discussed in Section 5.2 below.

The statistics described in this section so far are equally applicable to one-mode and two-mode (bipartite) graphs. When dealing with bipartite graphs, however, it is often useful to consider statistics of the two node sets separately. Hence we also define

$$z_{\text{BipartiteFourCyclesNodePowerA}}(\alpha) = \sum_{i \in A} [C_4(i)^\alpha] \quad (8)$$

and

$$z_{\text{BipartiteFourCyclesNodePowerB}}(\alpha) = \sum_{j \in B} [C_4(j)^\alpha] \quad (9)$$

for the two node sets A and B respectively. Because the sets A and B are disjoint, we have

$$z_{\text{FourCyclesNodePower}}(\alpha) = z_{\text{BipartiteFourCyclesNodePowerA}}(\alpha) + z_{\text{BipartiteFourCyclesNodePowerB}}(\alpha). \quad (10)$$

Representations of the new configurations are shown in Fig. 2. The vertical ellipsis \vdots in the figures is to indicate that the configuration includes any number (up to $\lfloor (n-1)/3 \rfloor$, since, apart from the one shared node, each four-cycle must include at most three distinct nodes) of four-cycles all involving a shared node (the central node in the figures).

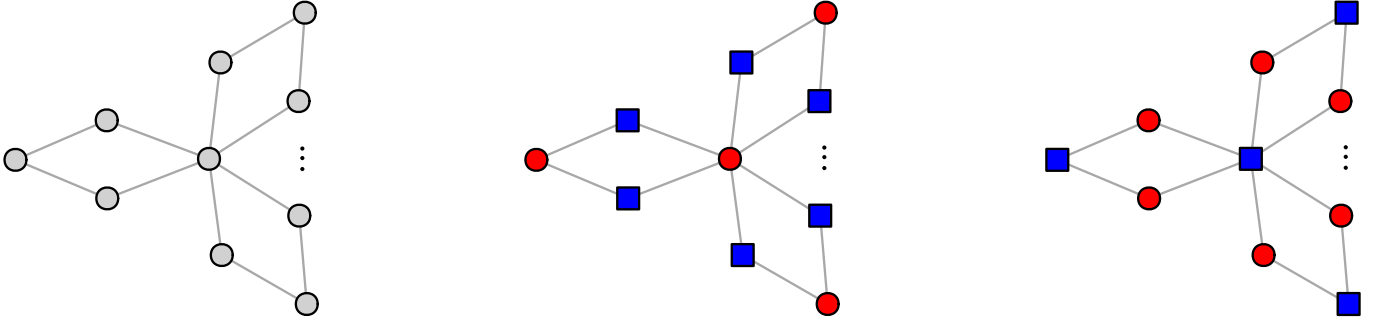


Figure 2: Representations of the new configurations (left to right) FourCyclesNodePower, BipartiteFourCyclesNodePowerA, and BipartiteFourCyclesNodePowerB. Nodes in node set A are shown as red circles, and nodes in node set B are shown as blue squares.

Table 3 shows the values of the BipartiteFourCyclesNodePowerA (BpNP4CA) and BipartiteFourCyclesNodePowerB (BpNP4CB) statistics for some small example bipartite networks, with the parameter $\alpha = 0.5$ (the alternating k -two-path statistics XACA and XACB are shown with their parameter $\lambda = 2.0$). Note that, unlike the XACA and XACB (K-C_A and K-C_P) statistics, these new statistics have the value zero for structures that contain no four-cycles (such as the two-path, ten-cycle, and nine-star structures in Table 3).

The “four-fan-3” graph in Table 3 is the same graph as the representation of the BipartiteFourCyclesNodePowerA configuration in Fig. 2 (ignoring the vertical ellipsis so that exactly three four-cycles are present). Note, however, that this has the counterintuitive property that, although it is a representation of the BipartiteFourCyclesNodePowerA configuration, in fact the value of the BipartiteFourCyclesNodePowerB statistic is greater than that of the BipartiteFourCyclesNodePowerA statistic for this graph. This is because the value of the statistic [(8) or (9)] is the sum over all nodes in the relevant node set (A or B , respectively) of the four-cycle count at each node (4) raised to the power α (“ α -inside” weighting). Therefore, in this graph, the nodes in mode B contribute more to the total as each one (of the six) is involved in exactly one four-cycle (and hence raising to the power of α still contributes one to the sum), while of the four nodes in mode A , three are involved in only one four-cycle, while the fourth is involved in three four-cycles and hence contributes only $3^\alpha \approx 1.73205$ (when $\alpha = 0.5$). Generalising this four-fan-3 graph to four-fan- k ($k \geq 1$, and if $k = 1$ the graph is just a four-cycle) with the central high-degree node in node set A , we have:

$$N_A = k + 1 \tag{11}$$

$$N_B = 2k \tag{12}$$

$$n = 3k + 1 \tag{13}$$

$$L = 4k \tag{14}$$

$$C_4 = k \tag{15}$$

$$\zeta_{\text{BipartiteFourCyclesNodePowerA}}(\alpha) = k^\alpha + k \tag{16}$$

$$\zeta_{\text{BipartiteFourCyclesNodePowerB}}(\alpha) = 2k \tag{17}$$

Because $0 < \alpha \leq 1$, the BipartiteFourCyclesNodePowerA statistic (16) will always be less than (or equal to, if $\alpha = 1$ or $k = 1$) the BipartiteFourCyclesNodePowerB statistic (17) for this family of graphs. The consequences for the interpretation of the corresponding parameters are discussed in Section 6.1.

5.1 Change statistics for the new statistics

The change statistic [25, 30, 40], that is, the difference in the statistic caused by adding a new edge (i, j) , for the four-cycles statistic (3) is

$$\delta_{C_4}(i, j) = \sum_{k \in N(i)} L_2(j, k) \tag{18}$$

$$= \sum_{k \in N(j)} L_2(i, k) \tag{19}$$

where $N(i)$ denotes the neighbours of node i , that is, nodes $k \neq i$ such that $x_{ik} = 1$, or, equivalently, $d(i, k) = 1$. The change statistic for the FourCyclesNodePower statistic (7) is then:

$$\begin{aligned} \delta_{\text{FourCyclesNodePower}(\alpha)}(i, j) &= [C_4(i) + \delta_{C_4}(i, j)]^\alpha - C_4(i)^\alpha \\ &+ [C_4(j) + \delta_{C_4}(i, j)]^\alpha - C_4(j)^\alpha \\ &+ \sum_{k \in N(i)} \left[(C_4(k) + L_2(k, j) + x_{kj}L_2(k, i))^\alpha - C_4(k)^\alpha \right] \\ &+ \sum_{\{k: k \in N(j) \wedge k \notin N(i)\}} \left[(C_4(k) + L_2(k, i))^\alpha - C_4(k)^\alpha \right]. \end{aligned} \quad (20)$$

The four terms in equation (20) count the contributions from, respectively, node i , node j , the neighbours of node i , and the neighbours of node j which are not also neighbours of node i . Note that in the third term (the contribution from neighbours of node i), a node k can only be a neighbour of both node i and node j (that is, $k \in N(i) \wedge x_{kj} = 1$) if the network is not bipartite.

The change statistic for the bipartite four-cycles statistic for the node set A (8) is simpler than the general case (20), as we only count the contributions from the nodes in node set A . Specifically, we have:

$$\begin{aligned} \delta_{\text{BipartiteFourCyclesNodePowerA}(\alpha)}(i, j) &= [C_4(i) + \delta_{C_4}(i, j)]^\alpha - C_4(i)^\alpha \\ &+ \sum_{k \in N(j)} \left[(C_4(k) + L_2(k, i))^\alpha - C_4(k)^\alpha \right] \end{aligned} \quad (21)$$

where $i \in A$, $j \in B$, and $k \in A$. The change statistic for BipartiteFourCyclesNodePowerB (9) is defined analogously.

5.2 Position of the new statistics in the dependence hierarchy

The configurations allowed in a model are determined by the assumptions as to which ties are allowed to depend on which other ties. Pattison & Snijders [22] (subsequently elucidated by Wang *et al.* [19] for bipartite networks, and more recently by Pattison *et al.* [77]) created a two-dimensional hierarchy of dependence assumptions, where the two dimensions are two facets of proximity: the form of the proximity condition, and the maximum distance between dependent ties. This two-dimensional hierarchy of dependence assumptions is illustrated in Fig. 3, showing a partial order structure, in which, if one dependence condition can be implied by another, it can be reached by a downwards path from the first to the second [19, p. 215].

In order to describe the proximity conditions, it is useful to define some notation for neighbourhoods in a graph. In Section 5.1 we defined $N(i)$ as the neighbours of node i , that is, nodes $k \neq i$ such that $d(i, k) = 1$. Following Pattison *et al.* [77], we now define $N_q(u)$, the q -neighbourhood of node u , as the set of nodes within geodesic distance q of u , that is, nodes v such that $d(u, v) \leq q$. Note that $N(u)$ as earlier defined in Section 5.1 is distinct from $N_1(u)$, the former being defined as nodes with a geodesic distance of exactly 1 from u (and hence excluding u itself), while the latter includes u itself as $d(u, u) = 0$. Further, we define $N_q(U)$, the q -neighbourhood of node set U , as $N_q(U) = \{v : v \in N_q(u) \text{ for some } u \in U\}$, that is, the set of nodes whose distance to some node in U is no more than q .

The four forms of proximity conditions, describing the nature of the proximity between the neighbourhoods of two pairs of nodes whose respective tie variables are hypothesized to be conditionally dependent only if the proximity condition holds, can be summarised as follows [77], in order of increasing generality:

1. Strict p -inclusion. SI_p ($p \geq 1$) holds if the p -neighbourhood of each node in a pair includes both of the nodes in the other pair.
2. p -inclusion. I_p ($p \geq 0$) holds if the p -neighbourhood of each pair of nodes includes the other pair.
3. Partial p -inclusion. PI_p ($p \geq 0$) holds if the p -neighbourhood of one pair of nodes includes the other pair.
4. p -proximity. D_p ($p \geq 0$) holds if the p -neighbourhood of one pair of nodes has a non-empty intersection with the other pair.

The dependence condition I_1 is equivalent to the widely-used ‘‘social circuit’’ dependence assumption [19], in which two ties are conditionally dependent if they would form a four-cycle if both present [30, 37, 78, 79], and PI_1 allows the ‘‘alternating pendant-triangle’’ statistics recently described by Pattison *et al.* [77].

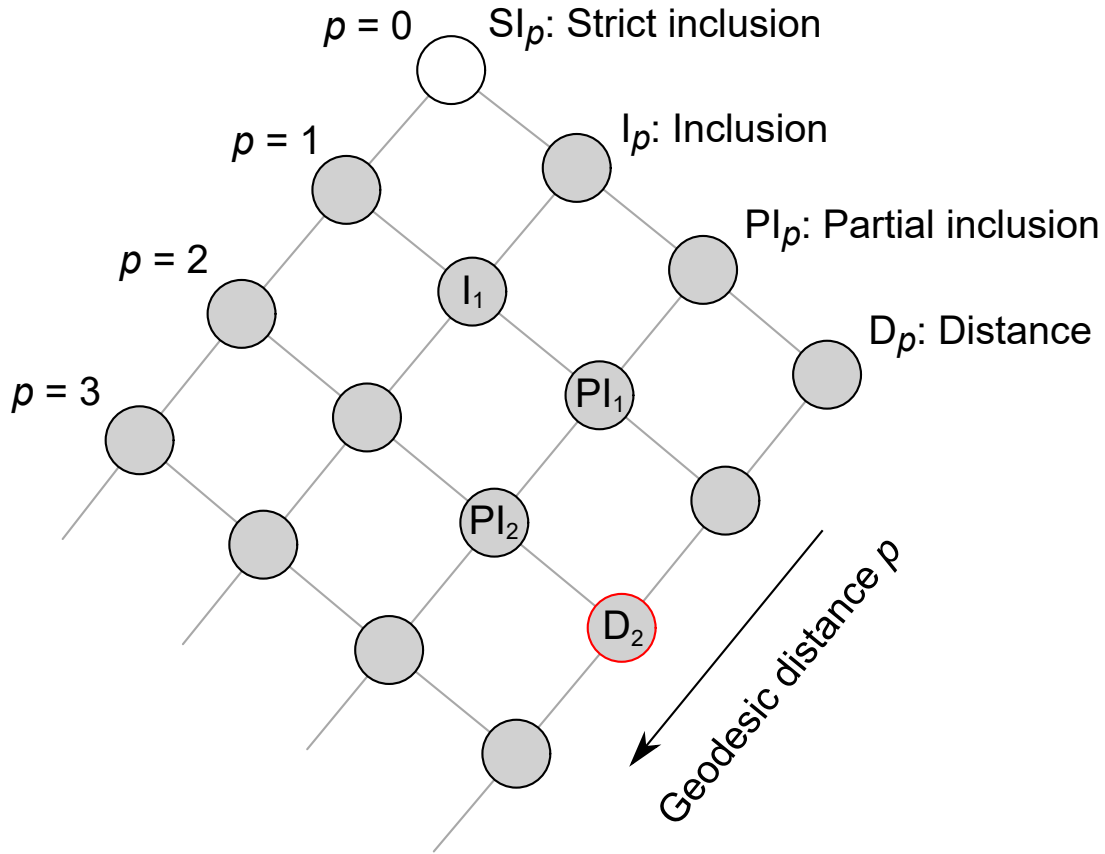


Figure 3: Dependence hierarchy, adapted from Wang *et al.* [19, Fig. 3]. SI_0 is not defined.

The change statistic for FourCyclesNodePower (20) in computing the probability of a new edge (i, j) , depends only on edges between nodes in the two-neighbourhoods of i and of j , since any two nodes in a four-cycle must be at a geodesic distance of at most two from each other (a four-cycle is a pair of nodes with two two-paths between them). Hence any edges on which the probability of edge (i, j) depend must be in the two-neighbourhood of $\{i, j\}$. This puts the FourCyclesNodePower configuration in the dependence class two-proximity (D_2): the p -neighbourhood (with $p = 2$) of one pair of nodes has a non-empty intersection with the other pair [22, 77]. D_2 is labelled with a red outline in the dependence hierarchy diagram shown in Fig. 3.

Because of the partial order structure of the dependence hierarchy, the stricter proximity forms for a fixed p imply the more general ones (and D_p is the most general), and for a fixed proximity condition, smaller p implies all the larger p (so D_1 implies D_2 for instance). Hence, to show that the FourCyclesNodePower configuration, which is in D_2 , is not also in any more specific dependence class, it is sufficient to show that it is not in D_1 and also not in PI_2 (see Fig. 3). To do so, we can use Proposition 3 of Pattison *et al.* [77], which gives the properties that must hold for configurations implied by the dependence structures associated with each proximity condition.

Proposition 3(d) of Pattison *et al.* [77] states that “For D_p , each configuration is a subgraph in which every pair of edges lies on a path of length $\leq (p+2)$ ” [77, p. 191]. So for a configuration to be in D_1 , every pair of edges must lie on a path of length three (or shorter). The FourCyclesNodePower configuration (Fig. 2) does not meet this requirement, since there are edges that do not lie on a path of length three or less: consider, for example, a pair of edges incident to the outermost node in the figure on two different four-cycles. These do not lie on a path of length three (but are on a path of length four, satisfying the requirement for D_2 but not D_1). Hence the FourCyclesNodePower configuration is not in dependence class D_1 .

Proposition 3(c) of Pattison *et al.* [77] states that “For PI_p , each configuration is a subgraph in which every pair of edges lies either on a cyclic walk of length $\leq (2p+2)$ or on a cyclic walk of length $\leq 2(p-r)+1$ with an additional path of length $\leq r+1$ attached to a node lying on the cyclic walk, for $0 \leq r \leq p-1$ ” [77, p. 191]. So, for PI_2 , each configuration is a subgraph in which every pair of edges is on a cyclic walk of length $\leq (2p+2) = 6$, or on a cyclic walk of length $\leq 2(p-0)+1 = 5$ with an additional path of length ≤ 1 attached to a node on the cyclic walk, or on a cyclic walk of length $\leq 2(p-1)+1 = 3$ with an additional path of length ≤ 2 attached to a node on the cyclic walk. Again, we can see that the configuration for FourCyclesNodePower does not meet these conditions, considering a

pair of maximally distant edges (those incident to the outermost nodes in two different four-cycles in Fig. 2). Such a pair of edges is neither on a six-cycle, and nor is it on a five-cycle with an additional path of length at most one or a three-cycle with an additional path of length at most two. Hence the FourCyclesNodePower configuration is not in dependence class PI_2 .

In the case of the BipartiteFourCyclesNodePower (A and B) statistics for bipartite networks, the same reasoning applies (see Fig. 2).

5.3 Implementation

The new ERGM effects FourCyclesNodePower, BipartiteFourCyclesNodePowerA, and BipartiteFourCyclesNodePowerB are implemented in the EstiNetDirected [71] software, available from <https://github.com/stivalaa/EstiNetDirected>. BipartiteFourCyclesNodePowerA and BipartiteFourCyclesNodePowerB are also implemented, as b1np4c and b2np4c, as user-contributed statnet model terms [80, 81], available from <https://github.com/stivalaa/ergm.terms.contrib>. An example is described in Appendix C.

The b1nodematch and b2nodematch statistics [21] are also implemented in EstiNetDirected (as BipartiteNodematchAlphaA, BipartiteNodematchAlphaB, BipartiteNodematchBetaA, and BipartiteNodematchBetaB). These statistics are described in Section 7.2.

To count the number of unique type A and B nodes that are involved in four-cycles in a two-mode network, the CYPATH software (<http://research.nii.ac.jp/~uno/code/cypath.html>) [82] was used to enumerate all of the four-cycles (which are necessarily chordless in a bipartite network).

Scripts for data conversion, statistical analysis, and generating plots were written in R [83] using the igraph [84,85] and ggplot2 [86] packages.

6 Simulation experiments

In order to investigate the effect of the BipartiteFourCyclesNodePowerA parameter, and compare it to that of the $K\text{-}C_A$ [18] (known as XACA in MPNet and BipartiteAltKCyclesA in EstiNetDirected) parameter, we conducted some simulation experiments. In these experiments, bipartite networks with 750 nodes in node set A and 250 nodes in set B were simulated with the Edge, BipartiteAltStarsA [$\lambda = 2$], and BipartiteAltStarsB [$\lambda = 2$] parameters set to -8.50 , -0.20 , and 2.00 , respectively. In one set of experiments, the BipartiteAltKCyclesA parameter was varied from -1.00 to 1.00 in increments of 0.01 , for each of three values of λ : 2, 5, and 10. In another set of experiments, the BipartiteFourCyclesNodePowerA parameter was varied from -1.00 to 2.00 in increments of 0.01 , for each of three values of α : $1/10$, $1/5$, and $1/2$. The networks were simulated using the SimulateERGM program from the EstiNetDirected software package, using the tie/no-tie (TNT) sampler [87], with a burn-in of 10^7 iterations and an interval of 10^5 iterations between each of 100 samples, to ensure that samples are drawn from the equilibrium ERGM distribution, and are not too autocorrelated.

The results of these simulations are shown in Fig. 4. Using the BipartiteAltKCyclesA parameter (left column) results in phase transition or near-degeneracy behaviour, with the statistic showing a sudden sharp increase at a critical value of the parameter. At this critical value, the graph density (top left plot) also sharply increases, as does the number of four-cycles (bottom left plot), which, at parameter values less than the critical value, hardly increased at all. This behaviour is similar to that of the simple Markov (edge-triangle) model described in Koskinen & Daraganova [37], and is characteristic of near-degeneracy in ERGMs. This can prevent estimation of models which contain parameters that cause this behaviour, and yet occurs in this case even when using an ‘‘alternating’’ statistic, designed to try to avoid such behaviour [18]. Note that changing the λ parameter appears merely to change the maximum value of the statistic; it does not remove or ‘‘smooth out’’ the phase transition. In contrast, when using the new BipartiteFourCyclesNodePowerA parameter (right column) the phase transition behaviour is less apparent even for the highest value of α ($1/2$), and can be smoothed out further as we decrease α . So, by appropriately setting α , we can use the BipartiteFourCyclesNodePowerA parameter to generate smoothly varying numbers of four-cycles, without suddenly tipping from a low-density low-clustering regime to a high-density high-clustering regime with nothing in between, which did not seem to be possible on this example with the BipartiteAltKCyclesA parameter.

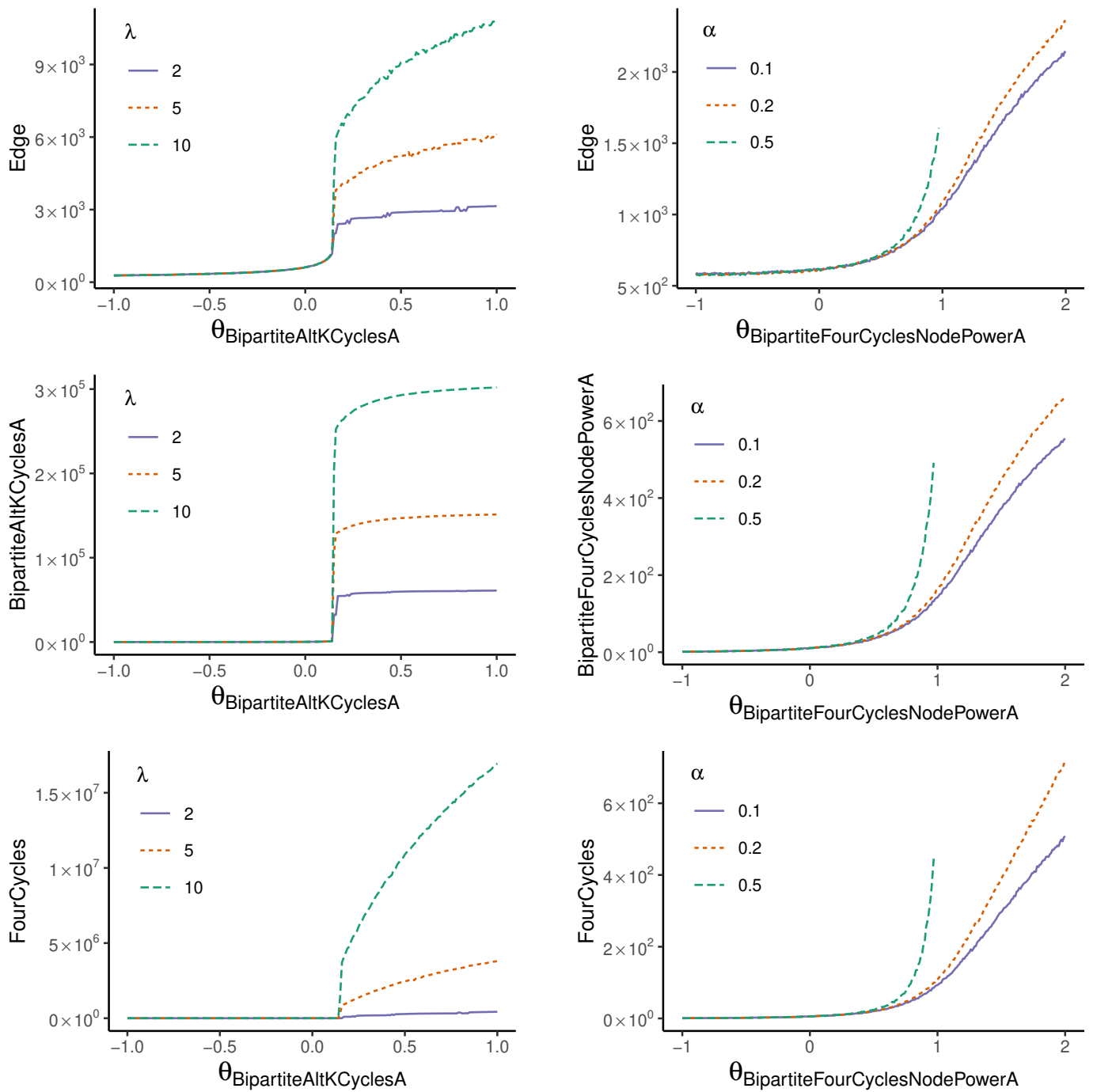


Figure 4: Effect of varying the BipartiteAltKCyclesA parameter (left) and BipartiteFourCyclesNodePowerA parameter (right) on the Edge statistic (top), the statistic corresponding to the parameter itself (middle) and the FourCycles statistic (bottom). Each graph plots the mean value of the statistic (over 100 simulated networks) for three different values of the λ or α parameter for BipartiteAltKCyclesA and BipartiteFourCyclesNodePowerA, respectively.

6.1 Interpretation of the new parameters

Interpretation of the `FourCyclesNodePower` parameter is that a positive value increases the number of four-cycles and a negative value decreases the number of four-cycles, relative to a value of zero. A smaller value of the exponent α means that additional four-cycles including the same node contribute less than if those cycles involved distinct nodes.

Interpretation of the `BipartiteFourCyclesNodePowerA` and `BipartiteFourCyclesNodePowerB` parameters is rather more complicated and is illustrated in Fig. 5 and Fig. 6. Note that in a bipartite network, any four-cycle must contain two nodes in node set A and two nodes in node set B . So how can we get more four-cycles in one mode than the other? The answer is that the four-cycle counts for the two must be equal, but the weighted node-oriented four-cycle counts (8) and (9) can differ. As discussed in Section 5, the statistic `BipartiteFourCyclesNodePowerA` (8) is maximised by having four-cycles involving distinct pairs of nodes in node set A (rather than many four-cycles involving the same node in node set A). If the `BipartiteFourCyclesNodePower` parameter for A is positive and for B is zero (or negative) then we tend to get more mode A nodes involved in four-cycles, with the same mode B nodes participating in many four-cycles, since the statistic is higher by having different nodes in the four-cycles, than for having the same node involved in many four-cycles. In the examples illustrated in Fig. 6, this results in the mode A nodes being part of a denser core with lots of four-cycles with a smaller number of B nodes, resulting in isolated B nodes. And vice versa for A zero (or negative) and B positive (“zero.pos” and “neg.pos”; these are perhaps clearer as there are more A nodes than B nodes in the network). Particularly in the “neg.pos” case, we can see a core of mode B nodes connected to a small number of central mode A nodes in four-cycles (as well as others not involved in four-cycles) and many mode A isolates. If `BipartiteFourCyclesNodePower` for both A and B are positive then there are even more four-cycles, but they are more evenly distributed between the A and B nodes.

Equation (10) implies that there are two degrees of freedom for the three parameters; for example we can include both `BipartiteFourCyclesNodePowerA` and `BipartiteFourCyclesNodePowerB` in a model, but not also `FourCyclesNodePower` since it is the sum of the other two.

7 Empirical applications

In this section we demonstrate the application of the new statistics in ERGM models of a selection of empirical two-mode networks ranging in size from hundreds of nodes to hundreds of thousands of nodes. Network summary statistics of the empirical networks are shown in Table 4 (four-cycle counts are shown in Table E1). The largest of these networks is larger than any of the networks in the literature survey (Table A1).

Table 4: Bipartite graph summary statistics. “Bipartite c.c” is the Robins-Alexander bipartite clustering coefficient [9].

Network	N_A	N_B	Mean degree		Bipartite c.c.
			A	B	
Inouye-Pyke pollinators	91	42	3.09	6.69	0.20856
St Louis crime	870	557	1.71	2.67	0.05041
Norwegian director interlock	1 495	367	1.23	5.00	0.09651
Robertson pollinators	1 428	456	10.68	33.45	0.10876
Australian director interlock	9 971	2 087	1.35	6.45	0.08438
Scientific collaborations	16 726	22 015	3.50	2.66	0.22822
International director interlock	321 869	34 769	1.17	10.84	0.12617

Three of the empirical network examples are director interlock networks [88], where nodes represent directors and companies, with an edge indicating that a director sits on a company board. Two of the empirical network examples are plant-pollinator webs, where edges represent an interaction between a plant and a pollinator, one network represents participation of actors in crime events, and one network represents scientific collaboration (co-authorship of scientific papers).

All of the ERGM models in this section were estimated with `EstimNetDirected` [71] using the simplified EE algorithm [28] with the improved fixed density (IFD) sampler [26] with 64 parallel estimation runs. Only models in which all runs converge and for which the model is non-degenerate (the observed statistics for effects in the model are within the 95% region of statistics simulated from the model) are presented. Simulations from the estimated models, used for the degeneracy check and goodness-of-fit testing, were done with the `SimulateERGM` program from the

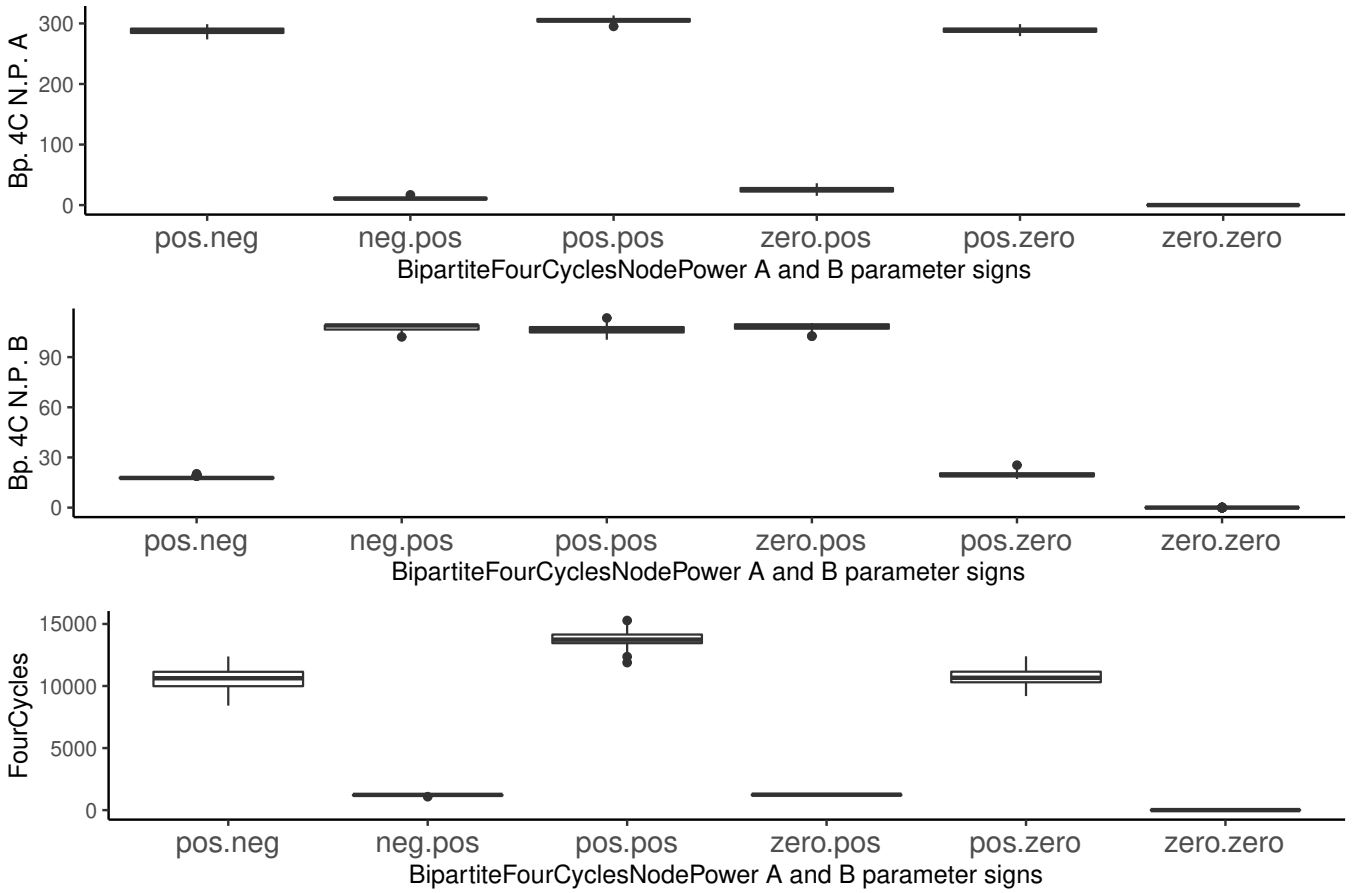


Figure 5: Effect of different combinations of negative, zero, and positive values of the BipartiteFourCyclesNodePowerA and BipartiteFourCyclesNodePowerB parameters on (top to bottom) the BipartiteFourCyclesNodePowerA statistic, the BipartiteFourCyclesNodePowerB statistic, and the FourCycles statistic. Box plots show the statistics of 100 simulated networks. The simulated bipartite networks have 100 nodes in node set A and 50 nodes in node set B and are simulated with common parameters (Edge, BipartiteAltStarsA [$\lambda = 2$], BipartiteAltStarsB [$\lambda = 2$]) = (-6.0, -0.4, 1.0). For BipartiteFourCyclesNodePowerA [$\alpha = 1/5$] and BipartiteFourCyclesNodePowerB [$\alpha = 1/5$] the negative (“neg”) parameter value is -1.5 and the positive (“pos”) parameter value is 6.5.

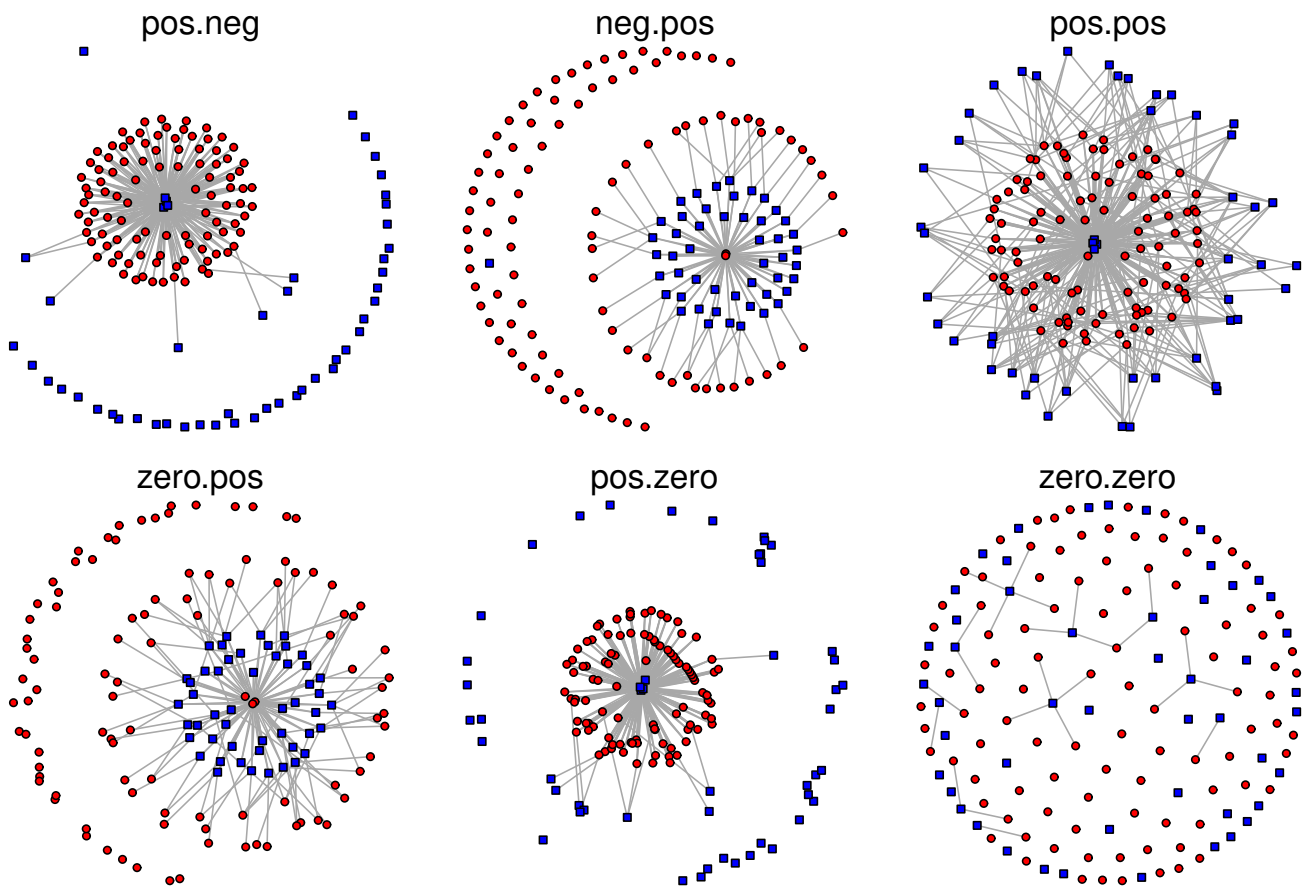


Figure 6: Examples of networks simulated with different combinations of negative, zero, and positive values of the BipartiteFourCyclesNodePowerA and BipartiteFourCyclesNodePowerB parameters, drawn from the simulations shown in Fig. 5. Nodes in node set A are shown as red circles, and nodes in node set B are shown as blue squares.

EstimNetDirected software package, with the tie/no-tie (TNT) sampler [87], with the exception of the Inouye-Pyke pollinator web, in which the IFD sampler was used.

7.1 Inouye-Pyke pollinator web

The Inouye-Pyke pollinator web [89] data was downloaded from the Interaction Web Database (IWDB) at https://www.nceas.ucsb.edu/interactionweb/html/inouye_1988.html (accessed 5 June 2018). (Note that the IWDB has since relocated and this data is now available from http://www.ecologia.ib.usp.br/iwdb/html/inouye_1988.html.) In this network, the node set A represents pollinators and node set B represents plants, and an edge represents an interaction between a pollinator and a plant.

Table 5 shows two ERGM models of Inouye-Pyke pollinator web. Model 1 includes the BipartiteAltKCyclesB term (models with BipartiteAltKCyclesA or FourCycles did not converge). Model 2 includes the new BipartiteFourCyclesNodePowerA and BipartiteFourCyclesNodePowerB terms. The former is found to be negative (but not statistically significant) while the latter is positive and statistically significant. This indicates a statistically significant tendency towards having multiple four-cycles involving distinct pairs of plants (node set B), and together with the negative or zero (not significant) BipartiteFourCyclesNodePowerA parameter, it models a network with pollinators (node set A) participating in multiple four-cycles. This is similar to the “zero.pos” or “neg.pos” case in Fig. 5 and Fig. 6, not coincidentally, since that simulation was based on this model.

Table 5: ERGM parameter estimates for the Inouye-Pyke pollinator web with 95% confidence intervals. Estimates in bold are statistically significant at this level. “Bipartite” in effect names is abbreviated to “Bp”.

Effect	Model 1	Model 2
Edge	-5.982 (-6.366, -5.598)	-6.229 (-6.470, -5.989)
BpAltStarsA [$\lambda = 2$]	0.923 (-0.552, 2.397)	-0.398 (-1.674, 0.878)
BpAltStarsB [$\lambda = 5$]	0.552 (-0.493, 1.597)	1.013 (0.319, 1.706)
BpAltKCyclesB [$\lambda = 2$]	0.005 (-0.322, 0.332)	—
BpFourCyclesNodePowerA [$\alpha = 1/5$]	—	-1.391 (-4.443, 1.662)
BpFourCyclesNodePowerB [$\alpha = 1/5$]	—	6.535 (1.670, 11.401)

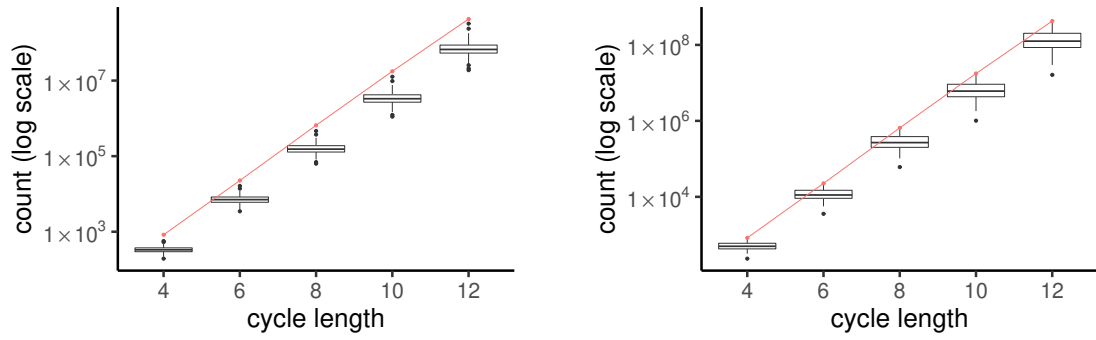
The positive and statistically significant BipartiteAltStarsB parameter indicates a tendency for centralisation on plant nodes, that is, plants that attract many pollinators.

The fit of the two models to the cycle length distribution of the network is shown in Fig. 7(a); Model 2 (right) has a slightly better fit to the distribution (and in particular four-cycles) than Model 1 (left). Fig. D1 shows more extensive goodness-of-fit plots for the two models. Model 2 has a better fit to all of the statistics included in the goodness-of-fit plots: degree distributions, giant component size, geodesic distance distribution, dyadwise shared partner distribution, and the bipartite clustering coefficients, as well as the cycle length distribution.

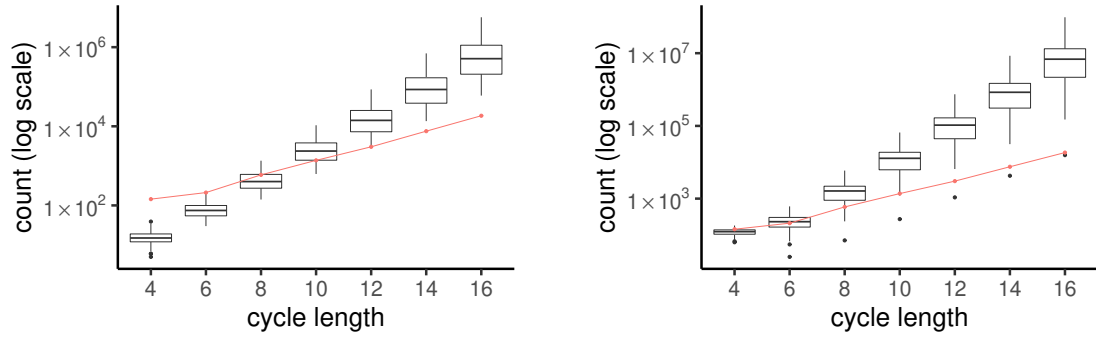
We also estimated Model 1 using MPNet (Table E2), and found the same parameter signs, but with smaller standard errors, so that XACB (BipartiteAltKCyclesB) is positive and significant, as are both XASA and XASB (BipartiteAltStarsA and BipartiteAltStarsB). This would appear to be a case of the EE algorithm (used in EstimNetDirected) having lower statistical power than the stochastic approximation algorithm [24] (used in MPNet) if an insufficient number of estimations runs are used [90, 91]. A positive and statistically significant estimate of the XACB parameter indicates a tendency for multiple pollinators to share the same plants (even in addition to the positive XASB (BipartiteAltStarsB) parameter indicating the presence of individual plant species that attract many pollinators).

7.2 St Louis crime network

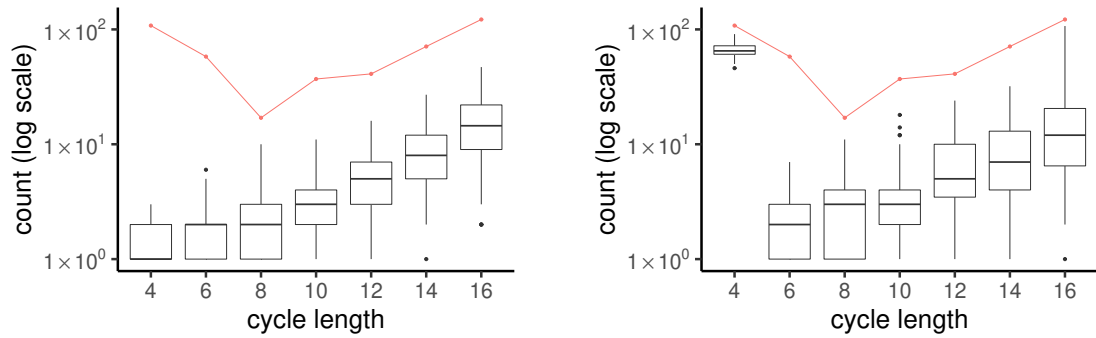
The St Louis crime network data [92] was obtained from the networkdata R package [93]. In this data, the nodes in node set A represent people, and the nodes in node set B represent crime events. In the original data, an edge can represent participation as a victim, suspect, witness or dual (both victim and suspect). Here, we consider any of these edge types to represent participation in the crime event. Individuals also have their gender recorded.



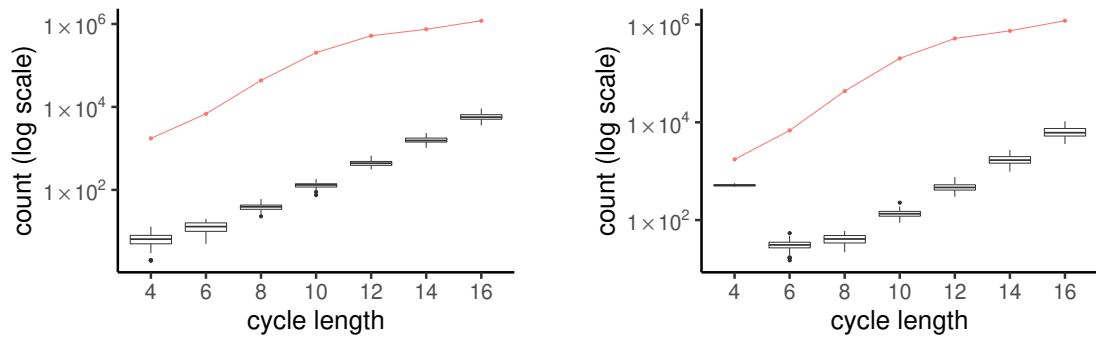
(a) Inouye-Pyke pollinators



(b) St Louis crime



(c) Norwegian director interlock



(d) Australian director interlock

Figure 7: Cycle length distribution goodness-of-fit plots for the empirical network examples. Plots in the left column are from models using the `BipartiteAltKCycles` parameter(s), where possible (no such model could be found for the St Louis crime network, so a simple model with no four-cycles effects is used), and plots in the right column are from models using the new `BipartiteFourCyclesNodePower` parameter(s). Observed network statistics are plotted as red points (joined by red lines as a visual aid) with box plots of the statistics of 100 simulated networks.

Four models of this network are shown in Table 6. Model 1 is a “baseline” model, with only edge, isolates, and star (degree distribution) effects. We were unable to find any converged models using the FourCycles or BipartiteAltK-Cycles (A or B) effects. Model 2 adds the BipartiteFourCyclesNodePower (A and B) effects. Fig. 7(b) shows the fit of Model 1 (left) and Model 2 (right) to the cycle length distribution of this network. Model 1 does not fit four-cycles well (but fits six-cycles, eight-cycles, and ten-cycles relatively well), while Model 2 fits four-cycles and six-cycles well, with the fit becoming progressively worse for longer cycle lengths (as it does for Model 1 with cycle lengths greater than ten).

More extensive goodness-of-fit plots for the two models are shown in Fig. D2. Model 2 fits well on all but geodesic distance distribution and giant component size. Notably it has better fit on the dyadwise shared partner distribution and the bipartite clustering coefficients than does Model 1, as a consequence of the former’s better fit to four-cycles.

Model 3 adds terms for gender homophily (including the term “BipartiteActivityA female” to capture a tendency for female actors to be more or less active in the network), while Model 4 adds terms for differential homophily on gender, that is, different homophily terms for male and female actors. BipartiteNodematchA [β] and BipartiteNodematchB [β] are the same as the statnet terms $b1nodematch(\beta)$ and $b2nodematch(\beta)$, as defined in Bomiriya *et al.* [21], for modelling homophily from an edge-centred view, in bipartite networks. The $b1nodematch(\beta)$ term is described by the *ergm* R package documentation as “half the sum of the number of two-paths with two first-mode nodes with that attribute as the two ends of the two path raised to the power β for each edge in the network” [48, ‘ $b1nodematch-ergmTerm$ ’], in other words, equation (7) of Bomiriya *et al.* [21]. This homophily statistic is edge-centred, as for every edge in a bipartite network, it counts the number of matching two-stars containing the edge (that is, pairs of nodes in one mode with the same attribute value that are connected to a common node in the other mode via a two-path containing that edge). This count for each such pair of nodes is then raised to the power β , and the sum is divided by two since each two-path contains two edges [21, p. 6]. Using these terms instead of measuring homophily in a more straightforward way by simply counting the number of two-paths between nodes with the same value of an attribute is advantageous for the two reasons discussed in Bomiriya *et al.* [21, p. 5]. First, the diminishing returns of additional two-paths connecting a pair of nodes with the same attribute that are already connected by a two-path means the $b1nodematch(\beta)$ term may be more appropriate from a modelling perspective, and, second, the simple two-path counting method can lead to problems of model degeneracy, which is alleviated by the use of an appropriate exponent β in the $b1nodematch(\beta)$ term.

The only effects that are found to be statistically significant (other than Edge) are BipartiteIsolatesA and BipartiteAltStarsA. The negative value of the former is likely a reflection of how the network was constructed: isolated people nodes are unlikely to occur as the network was constructed by a snowball sampling process from an initial set of crime reports. The positive value of the latter confirms a centralisation effect on person nodes, that is, there are people who are involved in a disproportionately large number of crime events. (There is no significant such effect for crime nodes, that is, crimes involving a disproportionately large number of people). None of the gender-related parameters are statistically significant, so we cannot draw any conclusions from this model as to the influence of gender in this network.

7.3 Robertson pollinator web

The Robertson pollinator network [94,95] data was downloaded from the Interaction Web Database (IWDB) at http://www.ecologia.ib.usp.br/iwdb/html/robertson_1929.html (accessed 19 April 2022). The node set A represents pollinators and the node set B represents plants, with an edge representing a plant-pollinator interaction. We were unable to find any converged model for this network, even with only edge and alternating- k -star terms. One reason that this network could be problematic for ERGM modelling is that it has at least an order of magnitude higher bipartite density than the other networks (with the exception of the Inouye-Pyke pollinator web, which has only 133 nodes, while this network has 1 884 nodes); this is also evident in the order of magnitude higher mean degrees for the Robertson pollinator web (Table 4). ERGMs are typically applied to social networks which are (usually) sparse, especially in the case of large networks [71], and there can be difficulties in trying to estimate ERGM parameters if the network is too dense; for example the neural networks for which ERGM models could not be estimated in Stivala & Lomi [96] and Stivala [97] also have density and mean degree at least an order of magnitude larger than the other biological networks [97, Table 1], for which ERGMs could be estimated. In those cases, the problem was overcome by using either the “Tapered ERGM” [31, 35, 98] or the LOLOG model [59, 60].

Table 6: ERGM parameter estimates for the St Louis crime network with 95% confidence intervals. Estimates in bold are statistically significant at this level. “Bipartite” in effect names is abbreviated to “Bp”

Effect	Model 1	Model 2	Model 3	Model 4
Edge	-12.345 (-12.589, -12.102)	-11.587 (-11.825, -11.349)	-11.439 (-11.685, -11.193)	-10.974 (-11.226, -10.723)
BpIsolatesA	-7.524 (-10.449, -4.600)	-7.112 (-10.276, -3.948)	-7.110 (-10.335, -3.885)	-7.114 (-10.420, -3.809)
BpIsolatesB	-4.096 (-10.860, 2.668)	-3.955 (-10.767, 2.857)	-3.830 (-10.966, 3.306)	-3.495 (-10.700, 3.710)
BpAltStarsA [$\lambda = 2$]	3.317 (2.042, 4.592)	2.851 (1.443, 4.259)	2.848 (1.382, 4.314)	2.850 (1.362, 4.339)
BpAltStarsB [$\lambda = 2$]	0.739 (-0.709, 2.187)	0.499 (-0.981, 1.980)	0.521 (-1.004, 2.046)	0.450 (-1.147, 2.048)
BpFourCyclesNodePowerA [$\alpha = 1/5$]	—	0.446 (-2.615, 3.506)	0.447 (-2.664, 3.558)	0.444 (-2.709, 3.597)
BpFourCyclesNodePowerB [$\alpha = 1/3$]	—	1.510 (-0.582, 3.601)	1.508 (-0.625, 3.641)	1.515 (-0.659, 3.689)
BpActivityA female	—	—	-0.075 (-0.758, 0.608)	-0.570 (-2.385, 1.245)
BpNodematchA gender [$\beta = 0.1$]	—	—	-0.249 (-2.028, 1.530)	—
BpNodematchA female [$\beta = 0.1$]	—	—	—	0.063 (-1.580, 1.707)
BpNodematchA male [$\beta = 0.1$]	—	—	—	-0.776 (-3.435, 1.883)

7.4 Norwegian director interlock network

The Norwegian director interlock network data [99] was downloaded from the supporting website described in the paper (accessed 29 June 2020). Note that this website is apparently no longer available, but we have retained a copy of the data which we downloaded. In this data, the nodes in node set A represent company directors, and the nodes in node set B represent companies; an edge represents a director sitting on the board of a company. We use only the network for 1 August, 2009, as also done in Opsahl [10]. There is also an attribute for the gender of directors, and location data (postcode and city) for companies.

Table 7 shows four models of this network. Model 1 is a structural model using the `BipartiteAltKCyclesB` term (models with `BipartiteAltKCyclesA` did not converge), while Model 2 is a structural model using the `BipartiteFourCyclesNodePowerA` and `BipartiteFourCyclesNodePowerB` terms. Model 3 and Model 4 add terms for geographical and gender homophily, with Model 4 testing for differential homophily on gender. These models use the `BipartiteNodematchA` [β] and `BipartiteNodematchB` [β] terms, as discussed in Section 7.2. The only statistically significant parameters (apart from `Edge`) are `BipartiteAltStarsA` and `BipartiteFourCyclesNodePowerA` (although the latter is not significant in Model 4, where terms for differential gender homophily are introduced). The negative `BipartiteAltStarsA` parameter indicates a lack of centralisation on the director degree distribution. The positive `BipartiteFourCyclesNodePowerA` (and negative, but not statistically significant, `BipartiteFourCyclesNodePowerB`) parameter means that there is a tendency towards having more directors than boards involved in four-cycles, with the same company boards participating in multiple four-cycles.

The fit of Model 1 (left) and Model 2 (right) to the cycle length distribution of the network is shown in Fig. 7(c). Neither fit the distribution well, but Model 2 is far closer to fitting the number of four-cycles well than Model 1 is.

Further goodness-of-fit plots are shown in Fig. D3. Model 1 fits the degree distributions well, but is not good on giant component size, geodesic distance distribution, dyadwise shared partner distribution, and, as already described, cycle length distribution (and hence bipartite clustering coefficients). Model 2 improves on Model 1 by having far better fit on the dyadwise shared partner distribution and (as already discussed), the number of four-cycles, and hence also the Robins-Alexander (but not Opsahl) bipartite clustering coefficient.

7.5 Australian director interlock network

Australian company director data was obtained from the Thomson Reuters Connect 4 Boardroom database <https://www.thomsonreuters.com.au/en-au/products/connect4.html> (accessed 14 September 2022 via Swinburne University of Technology institutional subscription). This data includes information on the country, gender and age of directors, and which companies they are directors of. This data was joined with other data from the Australian Securities Exchange (ASX), specifically the company directory <https://www.asx.com.au/asx/research/ASXListedCompanies.csv> (accessed 5 October 2022) and the “foreign entity report” for September 2022 <https://www.asx.com.au/listings/listing-considerations/listing-requirements/foreign-entity-data> (accessed 23 October 2022). From these data sources, a director interlock network was constructed, with nodes in mode A representing directors, and nodes in mode B representing companies. This network is the director interlock network for all companies listed on the ASX (as of September 2022), and also contains node attributes for the gender, age, and country of residence of directors, and the industry group (GICS), listing date, market capitalisation, and foreign country incorporation of companies. This is the same data used in earlier work [100], where more details, including descriptive statistics and simpler ERGM models, can be found.

Table 8 shows three ERGM models of the Australian director interlock network. Model 1 and Model 2 include the `BipartiteAltKCyclesB` parameter (models containing `BipartiteAltKCyclesA` did not converge), while Model 3 includes the `BipartiteFourCyclesNodePowerA` and `BipartiteFourCyclesNodePowerB` parameters. Just as for the Norwegian director interlock network (Section 7.4), `BipartiteAltStarsA` is negative and significant in all models, `BipartiteAltKCyclesB` is not significant in models that contain it (Models 1 and 2), and `BipartiteFourCyclesNodePowerA` is positive and significant with `BipartiteFourCyclesNodePowerB` not significant in Model 3. Hence, just as for the Norwegian director interlock network, there is a tendency towards having more directors than boards involved in four-cycles, with the same company boards participating in multiple four-cycles.

Figure 7(d) shows the fit of Model 2 (left) and Model 3 (right) to the cycle length distribution. Neither fit the distribution well, but Model 3 (with the new `BipartiteFourCyclesNodePower` parameters) has a far better fit to the number of four-cycles than Model 2 (with `BipartiteAltKCyclesB`) does.

Further goodness-of-fit plots are shown in Fig. D4. Both models have reasonable fit to the degree and geodesic

Table 7: ERGM parameter estimates for the Norwegian director interlock network with 95% confidence intervals. Estimates in bold are statistically significant at this level. “Bipartite” in effect names is abbreviated to “Bp”.

Effect	Model 1	Model 2	Model 3	Model 4
Edge	2.200 (1.950,2.451)	2.893 (2.675,3.112)	2.709 (2.487,2.930)	1.376 (1.153,1.599)
BpAltStarsA [$\lambda = 2$]	-3.342 (-4.927,-1.758)	-3.658 (-5.320,-1.995)	-3.871 (-5.655,-2.087)	-3.872 (-5.675,-2.070)
BpAltStarsB [$\lambda = 2$]	-2.748 (-9.662,4.167)	-3.101 (-7.752,1.551)	-3.181 (-8.114,1.751)	-3.137 (-7.986,1.712)
BpAltKCyclesB [$\lambda = 5$]	0.001 (-0.467,0.470)	—	—	—
BpFourCyclesNodePowerA [$\alpha = 1/3$]	—	2.512 (0.660,4.364)	2.382 (0.070,4.693)	2.373 (-0.155,4.902)
BpFourCyclesNodePowerB [$\alpha = 1/3$]	—	-0.246 (-2.118,1.626)	-0.128 (-2.603,2.347)	-0.118 (-2.934,2.699)
BpActivityA female	—	—	0.476 (-0.796,1.747)	2.180 (-1.265,5.625)
BpNodematchA gender [$\beta = 0.1$]	—	—	0.287 (-2.511,3.085)	—
BpNodematchA female [$\beta = 0.1$]	—	—	—	-0.409 (-2.331,1.514)
BpNodematchA male [$\beta = 0.1$]	—	—	—	2.228 (-3.308,7.763)
BpNodematchB city [$\beta = 0.1$]	—	—	0.597 (-0.783,1.977)	0.597 (-0.835,2.029)

Table 8: ERGM parameter estimates for the Australian director interlock network with 95% confidence intervals. Estimates in bold are statistically significant at this level. “Bipartite” in effect names is abbreviated to “Bp”

Effect	Model 1	Model 2	Model 3
Edge	-3.494 (-3.603, -3.385)	-2.226 (-2.369, -2.083)	-1.486 (-1.634, -1.339)
BpAltStarsA [$\lambda = 1.1$]	-5.123 (-7.255, -2.991)	-5.124 (-7.952, -2.295)	-5.538 (-8.549, -2.528)
BpAltStarsB [$\lambda = 5$]	-0.484 (-1.806, 0.838)	-0.517 (-2.281, 1.248)	-0.807 (-1.658, 0.044)
BpAltKCyclesB [$\lambda = 5$]	-0.086 (-0.459, 0.286)	-0.071 (-0.577, 0.436)	—
BpFourCyclesNodePowerA [$\alpha = 1/4$]	—	—	2.200 (0.194, 4.206)
BpFourCyclesNodePowerB [$\alpha = 1/4$]	—	—	0.746 (-1.448, 2.939)
BpActivityA female	0.657 (-0.209, 1.524)	-0.640 (-1.788, 0.507)	-0.841 (-2.005, 0.323)
BpContinuousActivityA age	0.010 (0.001, 0.020)	0.010 (-0.002, 0.023)	0.010 (-0.003, 0.024)
BpActivityA country.Australia	-1.256 (-1.627, -0.884)	-1.258 (-2.001, -0.516)	-0.998 (-1.878, -0.117)
BpActivityB country.Australia	-0.844 (-2.104, 0.417)	-0.842 (-2.573, 0.889)	-0.835 (-2.528, 0.858)
BpActivityB industryGroup.Banks	0.523 (-1.615, 2.661)	0.516 (-2.558, 3.591)	0.436 (-2.339, 3.212)
BpActivityB industryGroup.Materials	-0.559 (-1.217, 0.099)	-0.559 (-1.440, 0.322)	-0.508 (-1.495, 0.479)
BinaryPairInteraction gender.F country.Australia	0.001 (-0.533, 0.535)	0.011 (-0.687, 0.708)	0.028 (-0.561, 0.616)
BinaryPairInteraction gender.F industryGroup.Banks	0.472 (-2.042, 2.985)	0.449 (-3.185, 4.083)	0.408 (-2.748, 3.563)
BinaryPairInteraction gender.F industryGroup.Materials	-0.471 (-1.478, 0.535)	-0.459 (-1.773, 0.855)	-0.441 (-1.820, 0.939)
Matching country	2.163 (0.804, 3.523)	2.162 (0.280, 4.043)	2.101 (0.089, 4.113)
BpContinuousActivityB ListingYear	-0.000 (-0.001, 0.001)	-0.000 (-0.002, 0.002)	-0.000 (-0.002, 0.002)
BpContinuousActivityB logMarketCap	0.072 (-0.011, 0.154)	0.071 (-0.037, 0.179)	0.072 (-0.048, 0.193)
BpNodematchA country [$\beta = 0.1$]	3.489 (0.827, 6.152)	3.494 (0.067, 6.921)	3.388 (-0.615, 7.390)
BpNodematchB country [$\beta = 0.1$]	-1.552 (-2.900, -0.204)	-1.551 (-3.358, 0.256)	-1.476 (-3.375, 0.423)
BpNodematchB industryGroup [$\beta = 0.1$]	1.731 (1.018, 2.443)	1.731 (0.794, 2.668)	1.409 (0.267, 2.550)
BpNodematchA gender [$\beta = 0.1$]	0.527 (-1.139, 2.193)	—	—
BpNodematchA female [$\beta = 0.1$]	—	0.597 (-1.562, 2.756)	0.577 (-1.689, 2.843)
BpNodematchA male [$\beta = 0.1$]	—	-1.374 (-4.166, 1.417)	-1.627 (-4.502, 1.247)

distance distributions. Model 3 (with the new BipartiteFourCyclesNodePower parameters) has a better fit to the dyadwise shared partner distribution, and, as a consequence of fitting four-cycles better than Model 2, a better (but still not good) fit on the Robins-Alexander bipartite clustering coefficient (but not the Opsahl clustering coefficient, which depends on fitting six-cycles well).

These models also reproduce the attribute effects found in the simpler ERGM models of this network described in Stivala *et al.* [100]. Older directors tend to be on more boards (positive and significant BipartiteContinuousActivityA age, although this is only significant in Model 1), directors resident in Australia tend to be on fewer boards than those that are not (negative and significant BipartiteActivityA country.Australia), directors tend to be resident in the same country as the country of incorporation of companies whose boards they sit on (positive and significant Matching country), and directors on a board tend to be from the same country (positive and significant BipartiteNodematchA country in Models 1 and 2).

Although the models in Stivala *et al.* [100] found that larger market capitalisation is associated with larger boards (positive and significant BipartiteContinuousActivityB logMarketCap) and that foreign incorporated boards tend to have more directors, the equivalent effects here are not significant (BipartiteContinuousActivityB logMarketCap is positive but not significant and BipartiteActivityB country.Australia is negative but not significant).

In Stivala *et al.* [100], the simple homophily term BipartiteTwoPathMatchingA was used to test for gender homophily, but none of the gender effects were statistically significant. Here we use instead the BipartiteNodematchA [β] term, as discussed in Section 7.2, to test for gender homophily (Model 1) and differential gender homophily (Models 2 and 3). Again, however, none of the gender effects are statistically significant.

Models with the simple BipartiteTwoPathMatchingB term to test for country and industry homophily on boards (that is, to test if boards in the same country or industry tend to share directors) did not converge, but this problem was solved by using the BipartiteNodematchB [β] term instead. The effect for industry group homophily is positive and significant in all models, confirming that companies in the same industry group tend to be connected by shared directors. The effect for country homophily is negative (and statistically significant in Model 1 only).

7.6 Scientific collaborations

The scientific collaboration data is a co-authorship network of preprints in the Condensed Matter section of the arXiv e-print archive [101–103]. The nodes in node set A represent authors, and the nodes in node set B represent papers, with an edge between two nodes representing authorship on a paper. The data was downloaded from <https://toreopsahl.com/datasets/#newman2001> (accessed 17 April 2024); note that we use the two-mode (bipartite) version of this network as used in Opsahl [10], rather than the one-mode projection onto authors as is frequently used.

Table 9 shows two ERGM models for this network. Model 1 is a baseline model with only Edge, IsolateEdges, and degree distribution (alternating k -star) parameters. Model 2 adds the BipartiteAltKCyclesB parameter. Models including the FourCycles or BipartiteAltKCyclesA parameters did not converge, and nor did models including the new FourCyclesNodePower, BipartiteFourCyclesNodePowerA or BipartiteFourCyclesNodePowerB parameters.

Table 9: ERGM parameter estimates for the scientific collaboration network with 95% confidence intervals. Estimates in bold are statistically significant at this level. “Bipartite” in effect names is abbreviated to “Bp”.

Effect	Model 1	Model 2
Edge	-9.329 (-9.873, -8.785)	-10.462 (-10.752, -10.172)
IsolateEdges	1.033 (0.110, 1.956)	1.380 (0.438, 2.323)
BpAltStarsA [$\lambda = 2$]	1.028 (0.821, 1.234)	1.028 (0.820, 1.236)
BpAltStarsB [$\lambda = 2$]	-0.708 (-1.003, -0.412)	1.474 (0.830, 2.118)
BpAltKCyclesB [$\lambda = 5$]	—	-0.878 (-1.144, -0.611)

The positive and significant IsolateEdges parameter reflects the presence of more single-author papers than expected, given the other effects in the model, which include terms for the numbers of authors per paper and numbers of papers per author.

The negative and significant `BipartiteAltKCyclesB` parameter (in conjunction with the positive and significant `BipartiteAltStarsB` parameter reflecting the existence of papers with many authors) indicates that there is a tendency against multiple authors being on multiple papers together. Similar to the situation described for the top 500 Australian listed companies director interlock network described by Wang *et al.* [18, pp. 23–24], this, together with the presence of authors with many papers (positive and significant `BipartiteAltStarsA` parameter) suggests that there are highly active authors who tend to be on papers that do not otherwise share authors.

The goodness-of-fit plots for these models (Fig. D5) show that they have reasonable fit on mode *B* (paper) degree, but poor on mode *A* (author) degree (for low degree). The models also do not fit well to the dyadwise shared partner distribution (they do not reproduce the long tail), cycle length distribution, or the bipartite clustering coefficients. Model 2, despite including the `BipartiteAltKCyclesB` parameter, does not fit the dyadwise shared partner or four-cycles distributions (and hence bipartite clustering coefficients) any better than the baseline Model 1.

This network is therefore an example where the bipartite alternating *k*-cycle parameters do not improve the fit to four-cycles, and neither do the new `BipartiteFourCyclesNodePower` parameters, as converged models with the latter could not be found.

7.7 International director interlock network

The international director interlock network described in Evtushenko & Gastner [104] was downloaded from [105]. In this network, nodes in node set *A* represent directors, nodes in node set *B* represent companies, and an edge represents a director sitting on the board of a company. Director nodes have attributes for age and gender, while company nodes have attributes for country, sector, industry, and number of employees. This data was also used in earlier work [100], in which the ERGM model shown as Model 1 in Table 10 was first presented.

Table 10 shows three models of this network. Model 1 reproduces the model described in Stivala *et al.* [100], but estimated with 64 parallel estimation runs, rather than the 20 used in Stivala *et al.* [100]. Model 2 adds homophily effects for country, industry and sector on companies, and gender on directors, while Model 3 further adds effects for differential gender homophily. In Stivala *et al.* [100], none of these effects could be included as models including any of the simple homophily parameters `BipartiteTwoPathMatchingA` and `BipartiteTwoPathMatchingB` would not converge. By using the `BipartiteNodematchB` [β] and `BipartiteNodematchA` [β] parameters instead (see Section 7.2), however, these homophily effects can be included in the model. None of the models contain any of the `FourCycles`, `BipartiteAltKCycles` or `BipartiteFourCyclesNodePower` effects, as models containing any of these parameters did not converge.

Just as for the Norwegian (Section 7.4) and Australian (Section 7.5) director interlock networks, the `BipartiteAltStarsA` parameter is negative and statistically significant, confirming a tendency against centralisation in the director degree distribution (number of boards a director sits on). In this network however, the `BipartiteAltStarsB` parameter is positive and statistically significant, implying that there is centralisation in the board degree distribution (boards that have large numbers of directors).

Goodness-of-fit plots for Model 3 are shown in Fig. D6. The model fits the degree distributions well, but not the other statistics (giant component size, dyadwise shared partner distribution, and cycle length distribution; the network is too large to test the fit to the geodesic cycle length distribution in reasonable time). Specifically, the model generates significantly fewer four-cycles than the observed network has, which is perhaps not surprising, as the model contains no terms to model four-cycles. This therefore shows that the international director interlock network contains significantly more four-cycles than expected, given the other effects included in the model, which includes terms for density, centralisation on degree, and gender, industry, and homophily effects.

Model 1 is no different from the model in Stivala *et al.* [100]. The statistically significant effects in this model confirm that older directors tend to be on more boards, companies in the personal goods industry tend to have larger boards, and men are less likely to be on boards in the personal goods industry. The corresponding tests for women in the oil and gas industry are not statistically significant.

All of the homophily effects added in Model 2 are positive and statistically significant. Companies in the same country are more likely to share directors than those that are not, as are companies in the same industry, and directors of the same gender are more likely to be on the same boards. Model 3 adds terms for differential gender homophily, and this effect is positive and statistically significant for female but not male directors.

Table 10: ERGM parameter estimates for the international director interlock network with 95% confidence intervals. Estimates in bold are statistically significant at this level. “Bipartite” in effect names is abbreviated to “Bp”

Effect	Model 1	Model 2	Model 3
Edge	-10.391 (-10.702,-10.080)	-9.979 (-10.248,-9.710)	-9.891 (-10.159,-9.623)
IsolateEdges	-0.087 (-0.380,0.205)	0.037 (-0.334,0.408)	0.026 (-0.320,0.372)
BpAltStarsA [$\lambda = 5$]	-2.676 (-2.963,-2.390)	-3.315 (-3.619,-3.010)	-3.309 (-3.612,-3.006)
BpAltStarsB [$\lambda = 5$]	0.466 (0.408,0.524)	0.349 (0.286,0.412)	0.343 (0.279,0.406)
BpActivityA female	0.051 (-0.074,0.176)	0.020 (-0.060,0.100)	-0.553 (-0.807,-0.300)
BpContinuousActivityA age	0.005 (0.002,0.008)	0.004 (0.001,0.007)	0.005 (0.002,0.008)
BpActivityB industry.Personal.Goods	0.208 (0.103,0.314)	0.237 (0.121,0.353)	0.219 (0.109,0.330)
BpActivityB sector.Oil.and.Gas	-0.012 (-0.031,0.008)	-0.032 (-0.059,-0.006)	-0.033 (-0.060,-0.006)
BinaryPairInteraction gender.Female sector.Oil.and.Gas	-0.101 (-0.237,0.034)	-0.089 (-0.198,0.020)	-0.073 (-0.166,0.020)
BinaryPairInteraction gender.Male industry.Personal.Goods	-0.387 (-0.553,-0.221)	-0.396 (-0.573,-0.219)	-0.372 (-0.543,-0.201)
BpNodematchB country [$\beta = 0.1$]	—	2.513 (2.231,2.794)	2.512 (2.220,2.804)
BpNodematchB industry [$\beta = 0.1$]	—	1.087 (0.765,1.408)	1.087 (0.756,1.417)
BpNodematchB sector [$\beta = 0.1$]	—	0.328 (0.148,0.507)	0.328 (0.147,0.509)
BpNodematchA gender [$\beta = 0.1$]	—	0.316 (0.146,0.486)	—
BpNodematchA female [$\beta = 0.1$]	—	—	1.159 (0.731,1.587)
BpNodematchA male [$\beta = 0.1$]	—	—	0.119 (-0.030,0.268)

7.8 Summary

Table 11 summarises the models estimated for the empirical networks. No model containing the FourCycles parameter could be estimated for any of the networks, and neither could any model containing the BipartiteAltKCyclesA parameter (and so no models containing both BipartiteAltKCycles parameters could be estimated). For four of the seven networks, a model containing BipartiteAltKCyclesB could be estimated. In contrast, for all four networks where models using the new BipartiteFourCyclesNodePower parameters could be estimated, both BipartiteFourCyclesNodePowerA and BipartiteFourCyclesNodePowerB parameters were included in the model. Although both methods (BipartiteAltKCycles and BipartiteFourCyclesNodePower) could be used in only four of the seven networks, they are not the same four: there is one case (Scientific collaborations, Section 7.6) where BipartiteAltKCycles could be used but not BipartiteFourCyclesNodePower, and one case where the reverse is true (St Louis crime, Section 7.2).

Table 11: Summary of models fit to empirical networks. “neg” and “pos” indicate negative and positive parameter estimates, respectively, with * indicating statistical significance, while “n.c.” indicates that no converged model could be found.

Network	BipartiteAltKCycles		BipartiteFourCyclesNodePower	
	A	B	A	B
Inouye-Pyke pollinators	n.c.	pos	neg	pos*
St Louis crime	n.c.	n.c.	pos	pos
Norwegian director interlock	n.c.	pos	pos*	neg
Robertson pollinators	n.c.	n.c.	n.c.	n.c.
Australian director interlock	n.c.	neg	pos*	pos
Scientific collaborations	n.c.	neg*	n.c.	n.c.
International director interlock	n.c.	n.c.	n.c.	n.c.

8 Conclusion

The existing parameters for modelling shared partners or four-cycles in ERGMs for two-mode networks frequently lead to convergence problems, especially when parameters for both modes are included in the model. A literature survey shows that, perhaps as a result, the majority of published ERGM models of two-mode networks do not include these parameters. In addition, the majority of published models do not include an assessment goodness-of-fit to four-cycles.

In this work, we defined new ERGM effects to explicitly model four-cycles, and in the case of two-mode networks, four-cycle counts for the two modes separately. Simulation experiments show that ERGMs using the new parameters are able to generate bipartite networks with smoothly varying numbers of four-cycles, where the existing parametrisations cannot.

The empirical value of the new parametrisation was demonstrated on seven empirical two-mode networks, ranging in size from hundreds of nodes to hundreds of thousands of nodes. Four of the seven networks could have models estimated with existing parameters, but in all four cases only the parameter for one of the two modes could be included. In all four cases where converged models could be estimated with the new parameters, the parameters for both modes could be included, and the fit to the four-cycle count was better than that for models using existing ERGM parameters, where these could be estimated. We failed to estimate ERGM models at all for two of the networks, and for one network a model could only be estimated using the existing parameters, and not with the new ones. The new parameters are therefore not a complete solution to the problem of estimating ERGM models of two-mode networks, but are complementary to existing parameters, and further work remains in improving the ability to fit four-cycles (and longer cycles) in bipartite networks with ERGM models.

These new parameters come with both conceptual and computational costs. The conceptual cost is having to use a more general dependence class in the dependence hierarchy, without an underlying theoretical justification. The social circuit dependence assumption has theoretical justifications, as does partial inclusion (PI_1) for pendant-triangle configurations [77], but we are forced to use the more general class D_2 simply by the dependency induced by the new configuration, without any theoretical basis. The computational cost is incurred by having to traverse the two-neighbourhood of a dyad in computing the change statistic, and even with precomputation of two-path counts [71], this can be prohibitively slow (or require impractical amounts of memory) on dense and/or high four-cycle count or

very large networks, or those with very high degree nodes, such as the Robertson pollinator network and international director interlock network.

Another shortcoming is the counterintuitive and possibly confusing interpretation of the new parameters for bipartite networks (`BipartiteFourCyclesNodePowerA` and `BipartiteFourCyclesNodePowerB`; see Section 6.1). The new parameter for one-mode networks (`FourCyclesNodePower`) is also applicable to two-mode networks but does not treat the modes separately, and is relatively straightforward to interpret simply as a four-cycle closure parameter, so one solution is to use this, but this could omit important differences in the modes in a two mode network. Even the relatively straightforward `gwdegree` parameter used in `statnet` causes significant confusion due to the counterintuitive meaning of its sign [75, 106–108]. Having to use such relatively complex statistics, such as alternating, geometrically weighted, or the “ α -outside” or “ α -inside” [76] weightings often solves the problem of near-degeneracy, but comes at the cost of making the statistics difficult to interpret [35, p. 400]. An alternative solution to the conceptual (and possibly computational) problem is to use instead the LOLOG model [59, 60] or tapered ERGM [31, 35, 98] where a simple four-cycle parameter is unlikely to cause near-degeneracy problems, much as they enable a simple triangle parameter in one-mode networks where alternating or geometrically weighted parameters are required in standard ERGMs [35, 59, 97]. LOLOG, however, does not (currently) handle bipartite networks [59, 109], while tapered ERGM has the advantage of being implemented in the `statnet` framework and can use any terms in the `statnet` `ergm` package.

One further shortcoming of the new parameters is that the weighting parameter α is fixed, and not estimated as part of the model. A potential avenue of future work is to explore the possibility of estimating this parameter in the context of a curved ERGM in the `statnet` `ergm` package.

One final potential avenue for future work is in fitting cycles of length larger than four in bipartite networks. It appears that sometimes fitting four-cycles better also fits longer cycles better, but sometimes it does not (Fig. 7). Of particular importance are six-cycles, which have been suggested as the basis (rather than four-cycles) for measuring closure in two-mode networks [10]. The dependence class required for the new statistics described in this work also admits six-cycles as configurations, however we did not attempt to fit models with six-cycles as a parameter. It seems likely that, like the simple four-cycles parameter, attempting to do so would lead to problems with near-degeneracy, necessitating the creation of another weighted configuration analogous to those defined here for four-cycles (which would then be in another, even more general, dependence class).

Funding

This work was supported by the Swiss National Science Foundation [grant number 200778].

Acknowledgements

This work was performed on the OzSTAR national facility at Swinburne University of Technology. The OzSTAR program receives funding in part from the Astronomy National Collaborative Research Infrastructure Strategy (NCRIS) allocation provided by the Australian Government, and from the Victorian Higher Education State Investment Fund (VHESIF) provided by the Victorian Government.

A Models contained in literature survey

The list of 117 models in 59 publications is shown in Table A1. This table shows, for each network for which one or more models are presented in a paper, the size of both node sets in the network (N_A is the number of nodes in node set A , and N_B the number of nodes in node set B), the method used to estimate the model(s) in the paper, and the number of models for the network. Note that, in the case of multiple models for the same data, only a single model is counted; this is commonly the case for a model shown as developed incrementally, from a simple baseline model, and including more effects in subsequent models. In such cases, we consider only the final model. Multiple models are counted for cases such as models estimated for the same network at different time points, or for the same node set but with different edge types.

Table A1: Models included in literature survey of bipartite ERGM applications

Citation	Network description	Network size		Estim. method	Num. models
		N_A	N_B		
[110]	Theatregoers and theatre performances	290	24	MPLE	1
[54]	Theatregoers and theatre performances	290	24	MPLE	1
[53]	Municipalities and public utilities	116	120	Bergm	1
[55]	Shareholder activists and firms	162	220	statnet	1
[111]	Organizations and projects	198	95	BPNet	4
[112]	Customers and products (cars)	5000	250	statnet	6
[113]	Affiliation network (club membership)	257	15	BPNet	1
[114]	Actors and issues in water policy	?	?	statnet	1
[115]	Software contributors and software bugs	72	737	BPNet	1
[116]	Lemur species and plant genera	55	590	statnet	1
[117]	Buyers and sellers in an online drug cryptomarket	706	57	statnet	1
[118]	Buyers and sellers in an online drug cryptomarket	706	57	statnet	1
[119]	Co-attendance of Soviet politicians at events	67	1816	MPLE	8
[120]	Climate change adaptation actors and issues	659	19	statnet	1
[121]	Patents and inventors (temporal)	78 412	126 388	statnet	1
[122]	Fruit-frugivore interactions (vertebrates and plants), Continuum	133	315	statnet	1
[122]	Fruit-frugivore interactions (vertebrates and plants), Fragment	54	58	statnet	1
[123]	Provincial and national organizations	29	52	statnet	1
[124]	Authors and papers	2 200	76	BPNet	1
[125]	University departments and specializations	101	77	MPNet	1
[126]	Policy actors and decision-making forums	109	84	statnet	1
[72]	Director interlock, largest 248 corporations by revenue in Australia	1 251	248	BPNet	1
[127]	Organizations and research projects	1 316	237	BPNet	2
[128]	Interest groups and lobbying coalitions	171	74	statnet	1
[129]	Characters and their groups in an online game	465	396	BPNet	7
[130]	Organizations and forums in watershed policy	?	?	statnet	1
[131]	Organizations and policy institutions	527	146	BPNet	1
[132]	Wikipedia articles and editors	14 292	249	statnet	1
[133]	Southern Women	18	14	statnet	1
[133]	World city network (global firms and cities)	100	315	statnet	1
[133]	Inventors and patents	10 251	8 206	statnet	1
[134]	Travel destination countries and attitudes towards them	47	22	statnet	1
[135]	Disaster response organizations and resource types	27	10	BPNet	3
[135]	Affected neighbourhoods and resource contacts	19	10	BPNet	4
[136]	EU parliamentary chambers and proposals	39	650	statnet	1
[137]	Collaborations for hazard mitigation	95	198	statnet	1

Table A1: Models included in literature survey of bipartite ERGM applications

Citation	Network description	Network size		Estim. method	Num. models
		N_A	N_B		
[138]	Online doctor-patient consultations	?	?	statnet	1
[139]	Actors and institutions in water management	167	220	BPNet	2
[56]	Actors and forums in adapting to sea-level rise	82	9	statnet	1
[56]	Actors and forums in adapting to sea-level rise	647	103	statnet	1
[140]	Voluntary collaborative project teams	170	124	BPNet	1
[141]	Aged care residents and group activities	35	563	statnet	1
[142]	Organizations and policy forums	52	16	BPNet	2
[143]	Stakeholders and committees/working groups	152	9	BPNet	2
[143]	Stakeholders and committees/working groups	180	9	BPNet	5
[144]	Stakeholders and forums in urban development	60	14	MPNet	1
[145]	Stakeholders and forums in myrtle rust response	259	12	MPNet	1
[146]	Actors and instruments in water policy	31	15	statnet	1
[147]	"Swinging" couples and venues	57	39	BPNet	1
[148]	Organizations and projects in EU conservation (UK)	120	46	BPNet	1
[148]	Organizations and projects in EU conservation (NL)	54	40	BPNet	1
[148]	Organizations and projects in EU conservation (PT)	156	63	BPNet	1
[148]	Organizations and projects in EU conservation (GR)	124	57	BPNet	1
[148]	Organizations and projects in EU conservation (RO)	119	48	BPNet	1
[148]	Organizations and projects in EU conservation (LV)	122	28	BPNet	1
[149]	Buyers and sellers in an online drug cryptomarket	3 542	463	statnet	1
[150]	Citations from web top-level domains to health agency websites	?	148	statnet	1
[151]	Stakeholders and resilience planning documents	?	39	statnet	1
[152]	Drivers and regime shifts in social-ecological systems	57	25	statnet	1
[153]	Actors and forums in collaborative governance regimes	400	57	statnet	3
[154]	Customers and car models	5 000	281	statnet	1
[155]	Participants in design crowdsourcing contests	3 462	96	statnet	1
[156]	Deforestation emissions reduction projects and countries	480	57	MPNet	1
[157]	Crime control bills and their sponsors	1 304	221	statnet	1
[158]	Employees and ideas in intraorganizational crowdsourcing (stage 1)	213	236	BPNet	3
[158]	Employees and ideas in intraorganizational crowdsourcing (stage 2)	685	578	BPNet	3
[158]	Employees and ideas in intraorganizational crowdsourcing (full)	768	640	BPNet	3
[18]	Southern Women	18	14	BPNet	1
[18]	Director interlock	366	50	BPNet	1
[18]	Director interlock	255	198	BPNet	1
[19]	Student activists youth leaders by event	14	49	BPNet	1
[19]	Student activists organization by event	23	49	BPNet	1
[159]	Participants and teams in online crowdsourcing	2 100	946	statnet	1
[160]	EU Parliamentarians and information sources	77	18	statnet	1
[161]	Individuals and teams in an online game	333	426	BPNet	1

B A simpler, but unsuccessful, new statistic

Wang *et al.* [18] define the alternating k -two-path statistics $K-C_A$ and $K-C_P$, implemented as $XACA$ and $XACB$ in `MPNet` [44, 45], and `BipartiteAltKCyclesA` and `BipartiteAltKCyclesB` in `EstimNetDirected` (<https://github.com/stivalaa/EstimNetDirected>):

$$z_{\text{BipartiteAltKCyclesA}}(\lambda) = \lambda \sum_{i \in B} \sum_{\{l \in B: l < i\}} \left[1 - \left(1 - \frac{1}{\lambda}\right)^{L_2(i,l)} \right] \quad (22)$$

where $\lambda > 1$ is the decay parameter, and $L_2(i, l)$ is the number of two-paths connecting i to l , as defined by equation (2) in the main text. The corresponding change statistic is [18]:

$$\delta_{\text{BipartiteAltKCyclesA}}(\lambda)(i, j) = \sum_{l \in B} \left[x_{il} \left(1 - \frac{1}{\lambda}\right)^{L_2(j,l)} \right] \quad (23)$$

$$= \sum_{l \in N(i)} \left(1 - \frac{1}{\lambda}\right)^{L_2(j,l)}. \quad (24)$$

The statistic and change statistic for `BipartiteAltKCyclesB` are defined similarly.

As discussed in the main text (Section 4), one problem with this statistic, particularly if used to model bipartite closure, is that it counts two-paths (as its highest-weighted term) and not just four-cycles, and hence open paths, or cycles of length greater than four, contribute to the statistic, even if there are no four-cycles at all. A simple solution to this problem, therefore, is to remove the first term and reverse the signs, so that it no longer counts open two-paths, but the first, positive, term actually counts four-cycles. We therefore define a new statistic `BipartiteAltK4CyclesA` as

$$z_{\text{BipartiteAltK4CyclesA}}(\lambda) = - \left(z_{\text{BipartiteAltKCyclesA}}(\lambda) - z_{\text{TwoPathsA}} \right), \quad (25)$$

and its change statistic

$$\delta_{\text{BipartiteAltK4CyclesA}}(\lambda)(i, j) = - \left(\delta_{\text{BipartiteAltKCyclesA}}(\lambda) - \text{deg}(i) \right) \quad (26)$$

where

$$z_{\text{TwoPathsA}} = \sum_{i \in B} \sum_{\{l \in B: l < i\}} L_2(i, l) \quad (27)$$

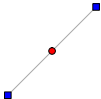
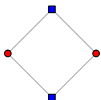
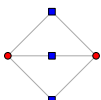
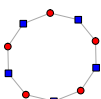
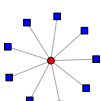
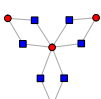
is the number of two-paths connecting nodes in node set B (and which therefore go through a node in node set A), and $\text{deg}(i)$, the degree of node i , is the change statistic for the number of two-paths through node i . `BipartiteAltK4CyclesB` and its change statistic are defined similarly. Unlike the new `FourCyclesNodePower` statistics defined in the main text (Section 5), these new statistics are in the same dependence class (I_1 , “social circuit”) as the original $K-C_A$ and $K-C_P$ statistics from which they are derived.

Table B1 is a copy of Table 3 in the main text, but with the new `BipartiteAltK4CyclesA` and `BipartiteAltK4CyclesB` statistics (labelled `BpAK4CA` and `BpAK4CB` respectively) included (and the N_A , N_B , L , `BpNP4CA`, and `BpNP4CB` columns removed to make space). This table shows the value of the new statistics on some small example networks, demonstrating, that, by design, they are zero for networks in which there are no four-cycles.

Unfortunately, however, simulation experiments indicate that the new `BipartiteAltK4CyclesA` and `BipartiteAltK4CyclesB` parameters are actually *more* problematic with respect to near-degeneracy than the original $K-C_A$ and $K-C_P$ parameters. Fig. B1 shows the results of simulation experiments similar to those described by Wang *et al.* [18, p. 19]. Bipartite networks were simulated with 30 nodes in node set A and 20 nodes in node set B with the Edge parameter set to -3.0 . In three different sets of simulations, for each of the `BipartiteAltKCyclesB`, `BipartiteAltK4CyclesB`, and `BipartiteFourCyclesNodePowerB` parameters, the parameter in question is varied from -1.00 to 10.0 in increments of 0.01 for each of two values of λ ($\lambda = 2$ and $\lambda = 5$) for `BipartiteAltKCyclesB` and `BipartiteAltK4CyclesB`, and for each of two values of α ($\alpha = 1/2$ and $\alpha = 1/5$) for `BipartiteFourCyclesNodePowerB`. The networks were simulated using the `SimulateERGM` program from the `EstimNetDirected` software package, using the basic ERGM sampler, with a burn-in of 10^5 iterations and an interval of 10^4 iterations between each of 100 samples, to ensure that samples are drawn from the equilibrium ERGM distribution, and are not too autocorrelated.

The top right panel in Fig. B1 shows the results of a simulation similar to that shown in Fig. 9 of Wang *et al.* [18]: the number of edges increases smoothly, giving good coverage of the graph space (with respect to density, at least).

Table B1: Statistics of some example bipartite networks. C_4 is the number of four-cycles, and $BpAK4CA$ and $BpAK4CB$ are the new statistics BipartiteAltK4CyclesA and BipartiteAltK4CyclesB, respectively. Nodes in node set A are represented as red circles, and nodes in node set B as blue squares.

Name	Visualization	C_4	XACA	XACB	$BpAK4CA$	$BpAK4CB$
Two-path		0	1	0	0	0
Four-cycle		1	1.5	1.5	0.5	0.5
Four-cycles-3		3	4.5	1.75	1.5	1.25
Ten-cycle		0	5	5	0	0
Nine-star		0	36	0	0	0
Four-fan-3		3	16.5	4.5	1.5	1.5

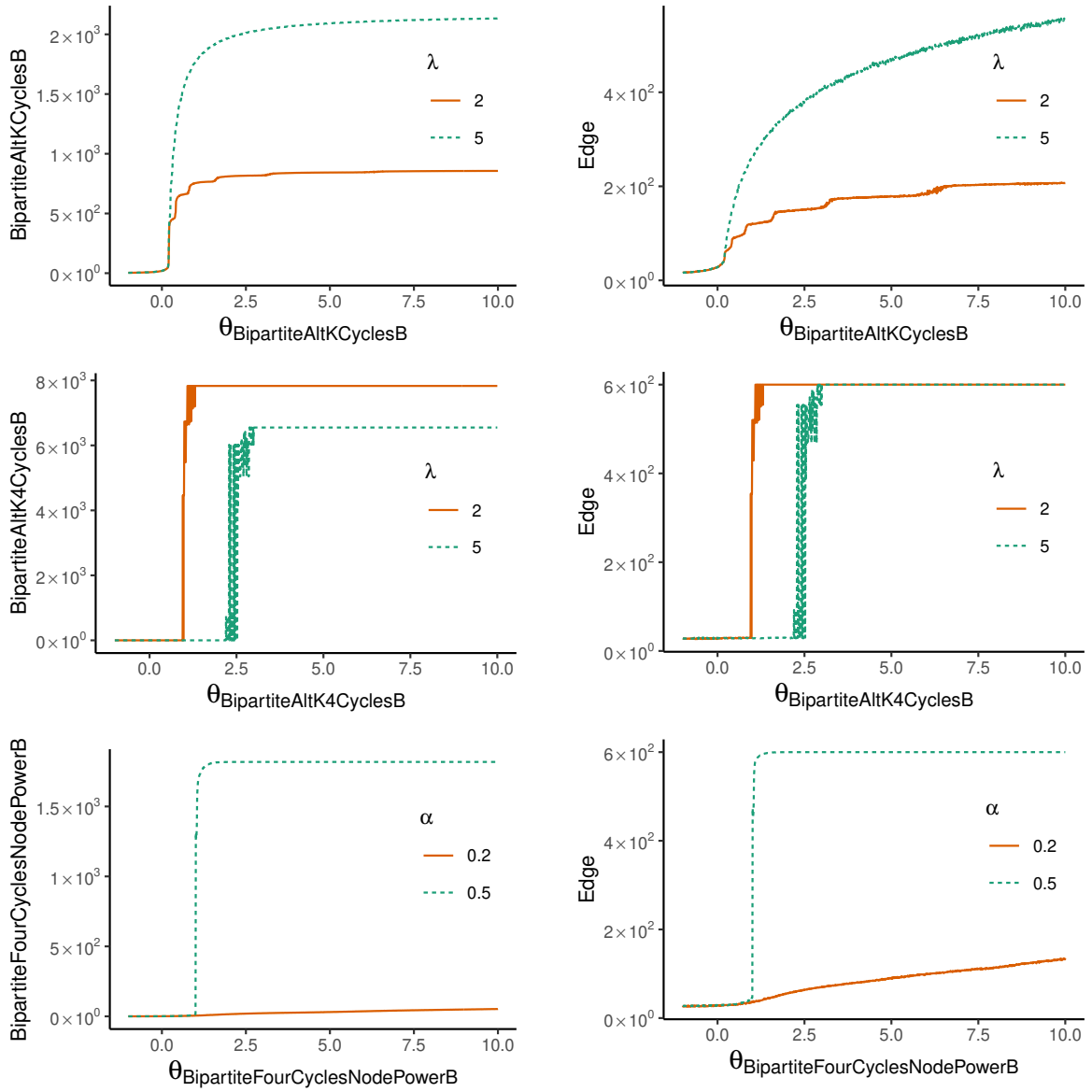


Figure B1: Effect of varying the BipartiteAltKCyclesB parameter (top), BipartiteAltK4CyclesB parameter (middle), and BipartiteFourCyclesNodePowerB parameter (bottom) on the statistic corresponding to the parameter itself (left) and the Edge statistic (right). Each graph plots the mean value of the statistic (over 100 simulations) for two different values of the relevant λ or α parameter.

The top left panel shows the value of the statistic corresponding to the parameter BipartiteAltKCyclesB itself. The behaviour of this curve is starting to look as if it could be prone to near-degeneracy, with a fairly steep increase at a critical value.

The graphs in the middle row of Fig. B1 show the results for the new BipartiteAltKCyclesB parameter. In this case, both the Edge statistic (right) and BipartiteAltK4CyclesB statistic itself (left) show a phase transition, where a critical value of the parameter separates an empty graph regime from a complete graph regime. This model is therefore near-degenerate, suggesting that this new parameter may in fact be less useful than the original $K-C_A$ and $K-C_P$ parameters.

For completeness, the bottom row of Fig. B1 shows the results for the new BipartiteFourCyclesNodePowerB parameter defined in the main text (Section 5). When $\alpha = 0.5$ an abrupt change from a near-empty to a full graph occurs, however, as shown by the result for $\alpha = 0.2$, this can be removed by decreasing the value of α .

Perhaps unsurprisingly, given the near-degeneracy demonstrated in Fig. B1, we were able to find a converged model with the new parameter for only one of the seven empirical networks described in the main text (Section 7). This is the smallest of the seven, the Inouye-Pyke pollinator web. Table B2 shows this model as Model 3 (Models 1 and 2 reproduce the models shown in Table 5 in the main text). Models with BipartiteAltK4CyclesA did not converge, and the value of λ for BipartiteAltK4CyclesB had to be reduced from the default ($\lambda = 2$) while the value of λ for

BipartiteAltStarsB had to be increased in order for this model to converge.

Table B2: ERGM parameter estimates for the Inouye-Pyke pollinator web. including Model 3 with the BipartiteAltK4Cycles parameter, with 95% confidence intervals. Estimates in bold are statistically significant at this level. “Bipartite” in effect names is abbreviated to “Bp”.

Effect	Model 1	Model 2	Model 3
Edge	-5.982 (-6.366, -5.598)	-6.229 (-6.470, -5.989)	-5.714 (-6.012, -5.416)
BpAltStarsA [$\lambda = 2$]	0.923 (-0.552, 2.397)	-0.398 (-1.674, 0.878)	—
BpAltStarsA [$\lambda = 5$]	—	—	0.497 (0.029, 0.965)
BpAltStarsB [$\lambda = 5$]	0.552 (-0.493, 1.597)	1.013 (0.319, 1.706)	0.495 (-0.024, 1.014)
BpAltKCyclesB [$\lambda = 2$]	0.005 (-0.322, 0.332)	—	—
BpFourCyclesNodePowerA [$\alpha = 1/5$]	—	-1.391 (-4.443, 1.662)	—
BpFourCyclesNodePowerB [$\alpha = 1/5$]	—	6.535 (1.670, 11.401)	—
BpAltK4CyclesB [$\lambda = 1.1$]	—	—	0.053 (0.004, 0.102)

The interpretation of Model 3 (Table B2) is similar to that of Model 1 and Model 2 discussed in Section 7.1. The positive and significant BipartiteAltStarsA parameter indicates centralisation on pollinator nodes, that is, the presence of pollinators that pollinate many plants. The positive and significant BipartiteAltK4CyclesB parameter indicates an over-representation of pollinators (node set A) participating in multiple four-cycles.

Goodness-of-fit plots for Model 3 are shown in Fig B2. Compared to the goodness-of-fit for Model 2 (Fig D1), the fit to the degree distribution for mode B nodes is worse, as is the fit to the geodesic distance distribution, however the fit to the cycle length distribution is slightly better, in particular for cycles of length 12.

In summary, we defined new BipartiteAltK4CyclesA and BipartiteAltK4CyclesB parameters as modified forms of the $K-C_A$ and $K-C_P$ parameters defined in Wang *et al.* [18], in order to count four-cycles but not open two-paths. However, near-degeneracy was exhibited in the simulation experiments (similar results occur with the larger simulated networks described in Section 6; data not shown), and a converged model using them could only be found for one of the seven networks tested. We conclude, therefore, that although these new parameters could potentially be useful in some cases, they are more prone to near-degeneracy and not as useful as either the existing $K-C_A$ and $K-C_P$ parameters, or the new BipartiteFourCyclesNodePowerA and BipartiteFourCyclesNodePowerB parameters described in the main text.

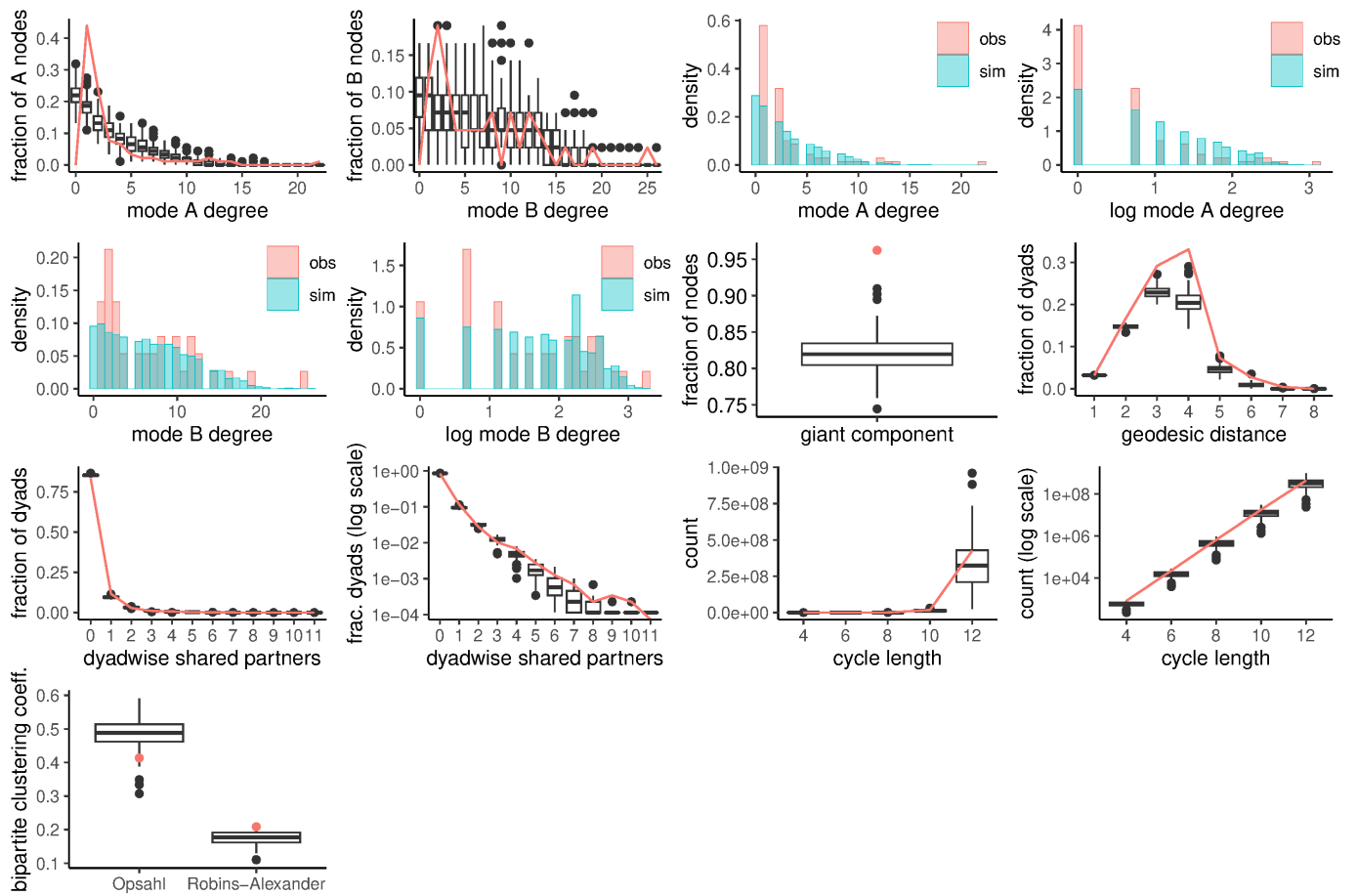


Figure B2: Goodness-of-fit plots for Inouye-Pyke pollinator web ERGM Model 3 (Table B2). The observed network statistics are plotted in red with the statistics of 100 simulated networks plotted as black box plots, and blue on the histograms.

C Statnet implementation example

The new statistics `BipartiteFourCyclesNodePowerA` and `BipartiteFourCyclesNodePowerB` were implemented in `statnet` as `b1np4c` and `b2np4c`, using the facility to define custom `ergm` model terms [80, 81]. They are available at <https://github.com/stivalaa/ergm.terms.contrib>.

Here we demonstrate this implementation by using the `statnet` `ergm` package [48] with the new user terms to estimate a model for the Davis “Southern Women” network [162], obtained via the `latentnet` R package [163, 164]. This well-known affiliation network represents the participation of 18 women (first mode) in 14 social events (second mode).

The `b1np4c` and `b2np4c` model terms take the α ($0 < \alpha \leq 1$) value as a parameter, with a default value of $\alpha = 0.5$ if omitted. For example, to estimate a model with the `b2np4c` (`BipartiteFourCyclesNodePowerB`) term with $\alpha = 1/5$ (Model 4 in Table C1):

```
davis_model4 <- ergm(davis ~ edges + gwbldegree(1, TRUE) +
                    gwb2degree(1, TRUE) + b2np4c(1/5),
                    control = control.ergm(main.method = "Stochastic-Approximation"))
```

Table C1: ERGM parameter estimates for the Southern Women network, estimated with `statnet`. The table was generated directly from the `statnet` models with the `texreg` R package [165].

	Model 1	Model 2	Model 3	Model 4
edges	−2.07*** (0.34)	−0.20 (0.24)	0.47 (0.31)	−5.90*** (0.58)
b1star2	0.07 (0.07)			
b2star2	0.18*** (0.04)			
gwb1deg.fixed.1		−0.83 (1.03)	−7.04*** (1.51)	10.60*** (1.80)
gwb2deg.fixed.1		−2.26** (0.85)	7.76** (2.48)	−6.95*** (1.57)
gwb1dsp.fixed.0.5			0.45*** (0.12)	
gwb2dsp.fixed.0.5			−1.33*** (0.30)	
b2np4c.fixed.0.2				17.30*** (1.86)
AIC	319.34	328.85	308.77	285.41
BIC	329.93	339.44	326.41	299.53
Log Likelihood	−156.67	−161.43	−149.38	−138.71

*** $p < 0.001$; ** $p < 0.01$; * $p < 0.05$

Table C1 shows four models for the Southern Women network, estimated with the stochastic approximation algorithm [24]. Model 1, with only the edges and two-star terms for each mode, is the same as [18, Model (8.3)]. Model 2, using the geometrically weighted degree terms rather than two-stars, is similar to [18, Model (8.5)], but using the `statnet` `gwbldegree` and `gwb2degree` terms rather than the `BPNet` alternating k -star terms $K-S_P$ and $K-S_A$. Note the reversal of interpretation of signs between $K-S_P/K-S_A$ and `gwbldegree/gwb2degree` [106, 107]. Model 3, adding the geometrically weighted dyadwise shared partner terms, is similar to [18, Model (8.6)]. Model 4 uses the new `b2np4c` term rather than the geometrically weighted dyadwise shared partner terms `gwb1dsp` and `gwb2dsp` (models with `b1np4c` did not converge).

Cycle length distribution goodness-of-fit plots for the four models are shown in Fig. C1, and `statnet` goodness-of-fit plots in Fig. C2. Note that all four models fit acceptably well on all the statistics included in the goodness-of-fit tests (degree distributions for each mode, dyadwise shared partners, and geodesic distance distribution), as well as the cycle length distributions. In particular, the fit to four-cycle counts is good for all models, including Model 1

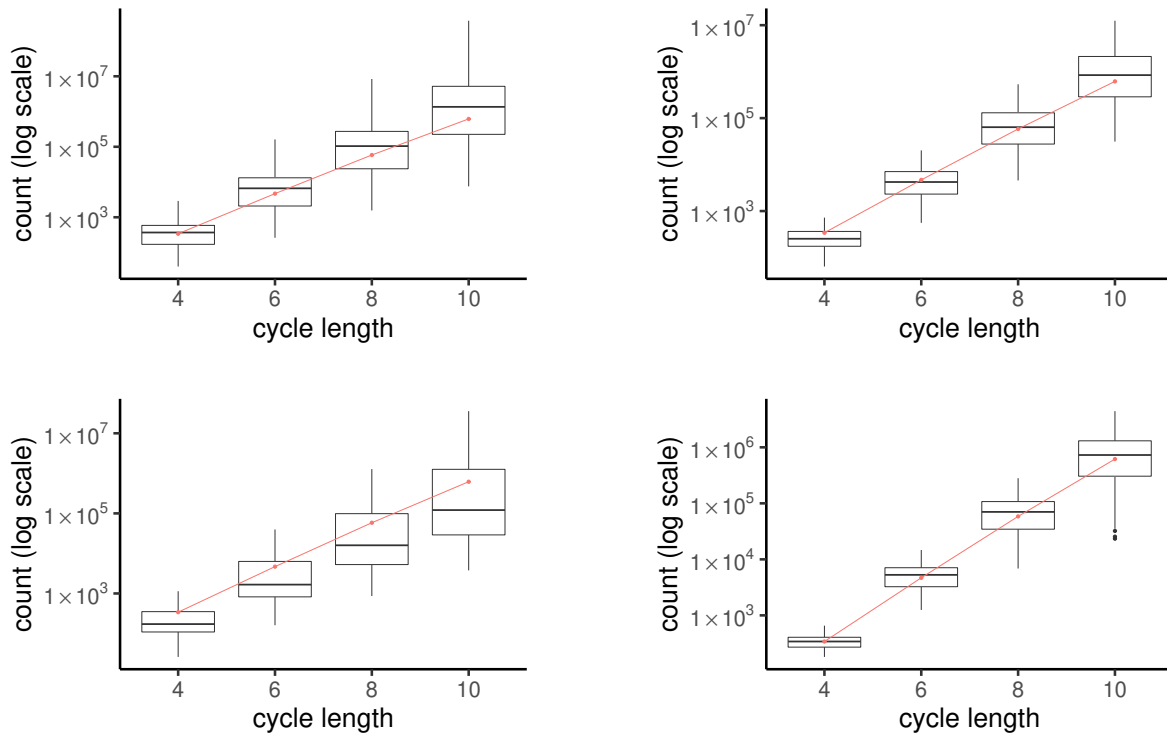


Figure C1: Cycle length distribution goodness-of-fit plots for the Southern Women network ERGM (Table C1) Model 1 (top left), Model 2 (top right), Model 3 (bottom left), and Model 4 (bottom right). Observed network statistics are plotted as red points (joined by red lines as a visual aid) with the statistics of 100 simulated networks plotted as black box plots.

and Model 2, which do not contain any terms to model four-cycles. It therefore appears that Model 1 is the most parsimonious explanation of this data, just as discussed in Wang *et al.* [18, pp. 22]. This model has a positive and statistically significant event two-star parameter (b_{2star2}), indicating “greater discrepancies in the popularity of events than expected in a random network” [18, pp. 22], taking into account the density (edges) and actor two-star (b_{1star2}) effects.

That ERGM models containing only terms to model density and degree distributions (and specifically not any terms to model dyadwise shared partner distributions or four-cycles) also fit the four-cycle count well indicates that the observed number of four-cycles could have occurred simply by chance [18, pp. 22]. Note that the same applies also to six-cycles. This is consistent with the results for this network described by Opsahl [10], where the observed value of the two-mode global clustering coefficient defined in that paper is not extreme in the distribution of that coefficient in random networks.

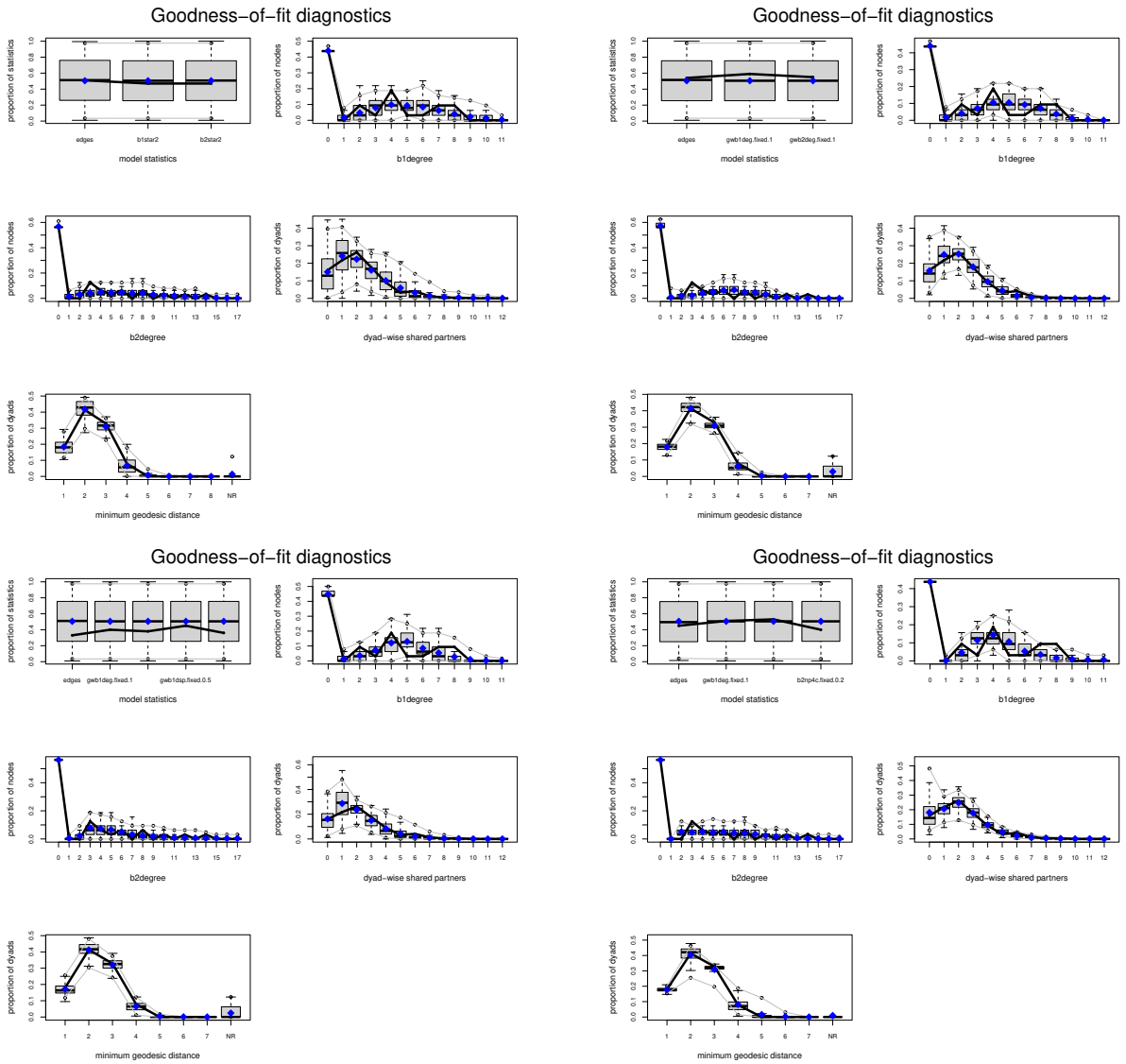


Figure C2: Statnet goodness-of-fit plots for the Southern Women ERGM (Table C1) Model 1 (top left), Model 2 (top right), Model 3 (bottom left), and Model 4 (bottom right).

D Goodness-of-fit plots

Goodness-of-fit plots for the ERGM models for the Inouye-Pyke pollinator web (Table 5), the St Louis crime network (Table 6), the Norwegian director interlock network (Table 7), the Australian director interlock network (Table 8), the scientific collaboration network (Table 9), and the international director interlock network (Table 10) are shown in Fig. D1, Fig. D2, Fig. D3, Fig. D4, Fig. D5, and Fig. D6, respectively.

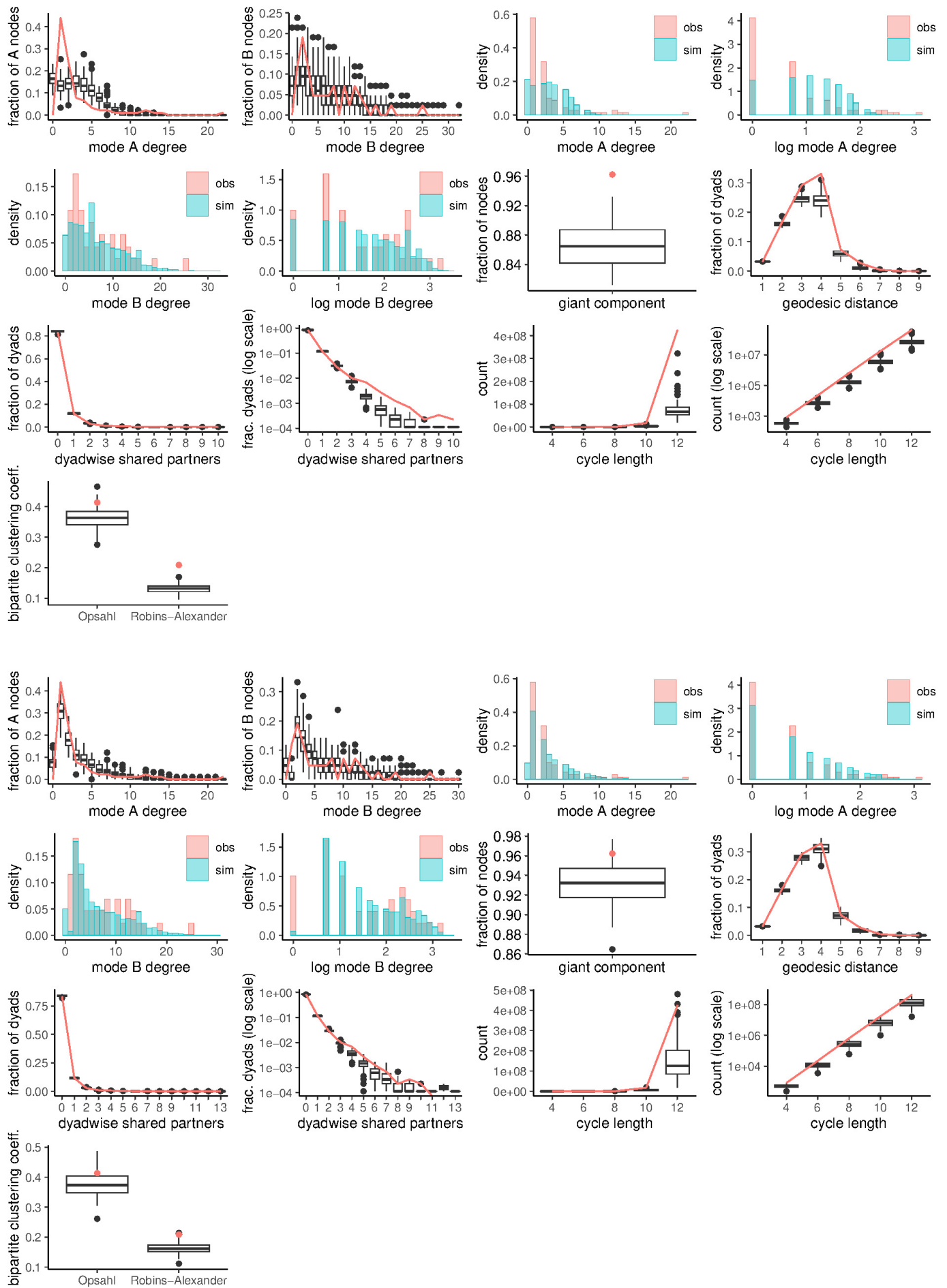


Figure D1: Goodness-of-fit plots for Inouye-Pyke pollinator web ERGM (Table 5) Model 1 (top) and Model 2 (bottom). The observed network statistics are plotted in red with the statistics of 100 simulated networks plotted as black box plots, and blue on the histograms.

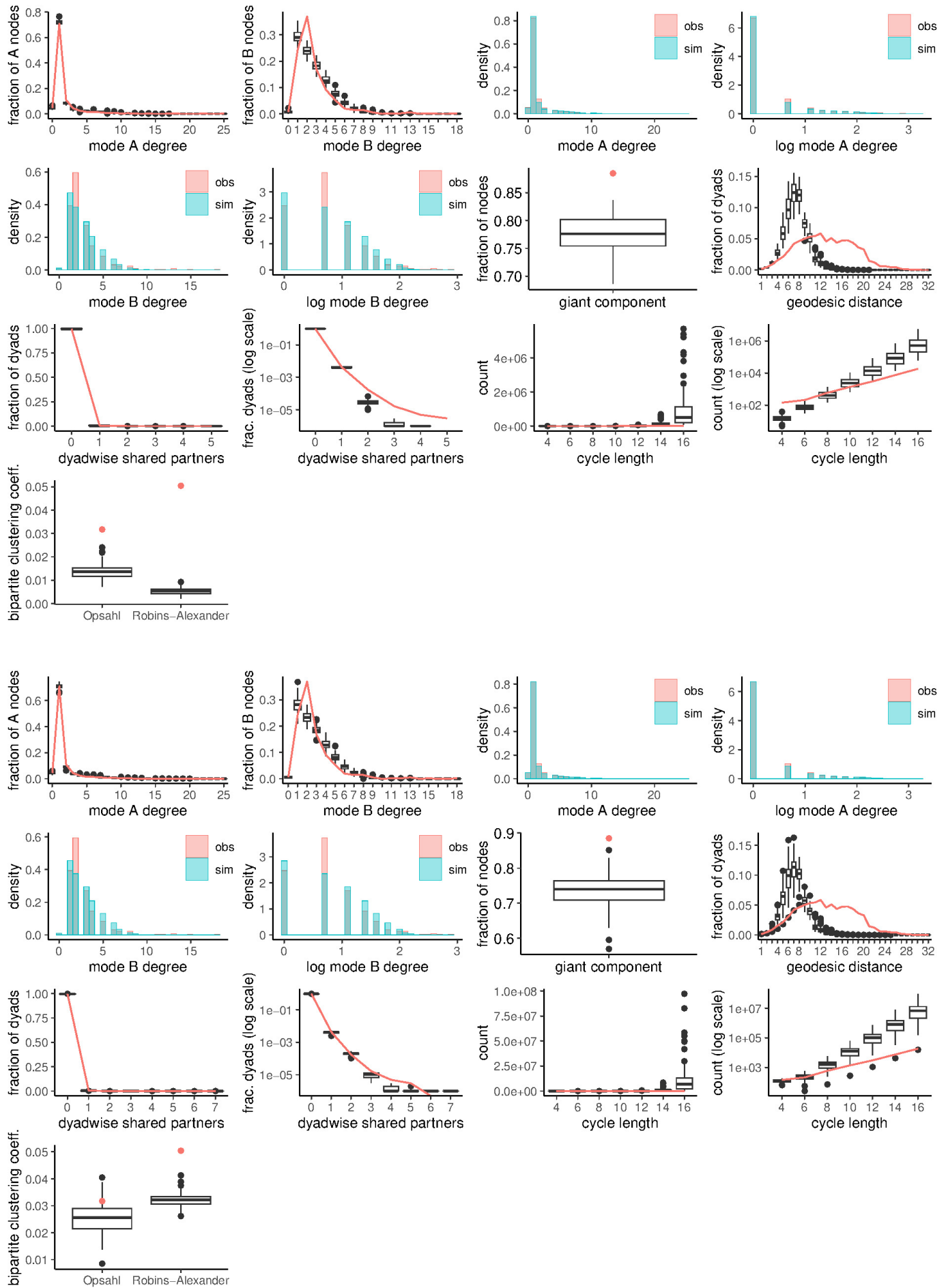


Figure D2: Goodness-of-fit plots for the St Louis crime network ERGM (Table 6) Model 1 (top) and Model 2 (bottom). The observed network statistics are plotted in red with the statistics of 100 simulated networks plotted as black box plots, and blue on the histograms.

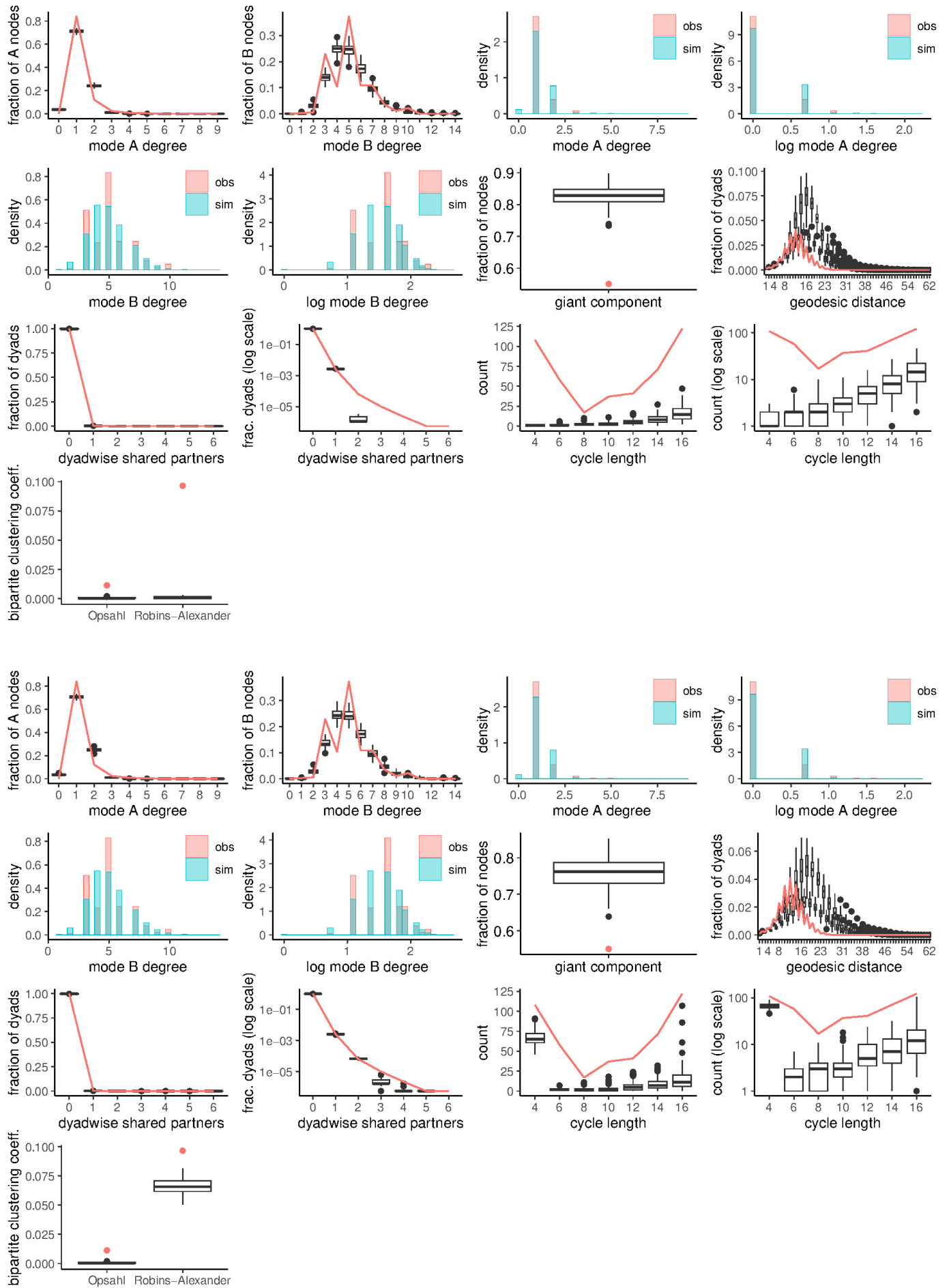


Figure D3: Goodness-of-fit plots for the Norwegian director interlock network ERGM (Table 7) Model 1 (top) and Model 2 (bottom). The observed network statistics are plotted in red with the statistics of 100 simulated networks plotted as black box plots, and blue on the histograms.

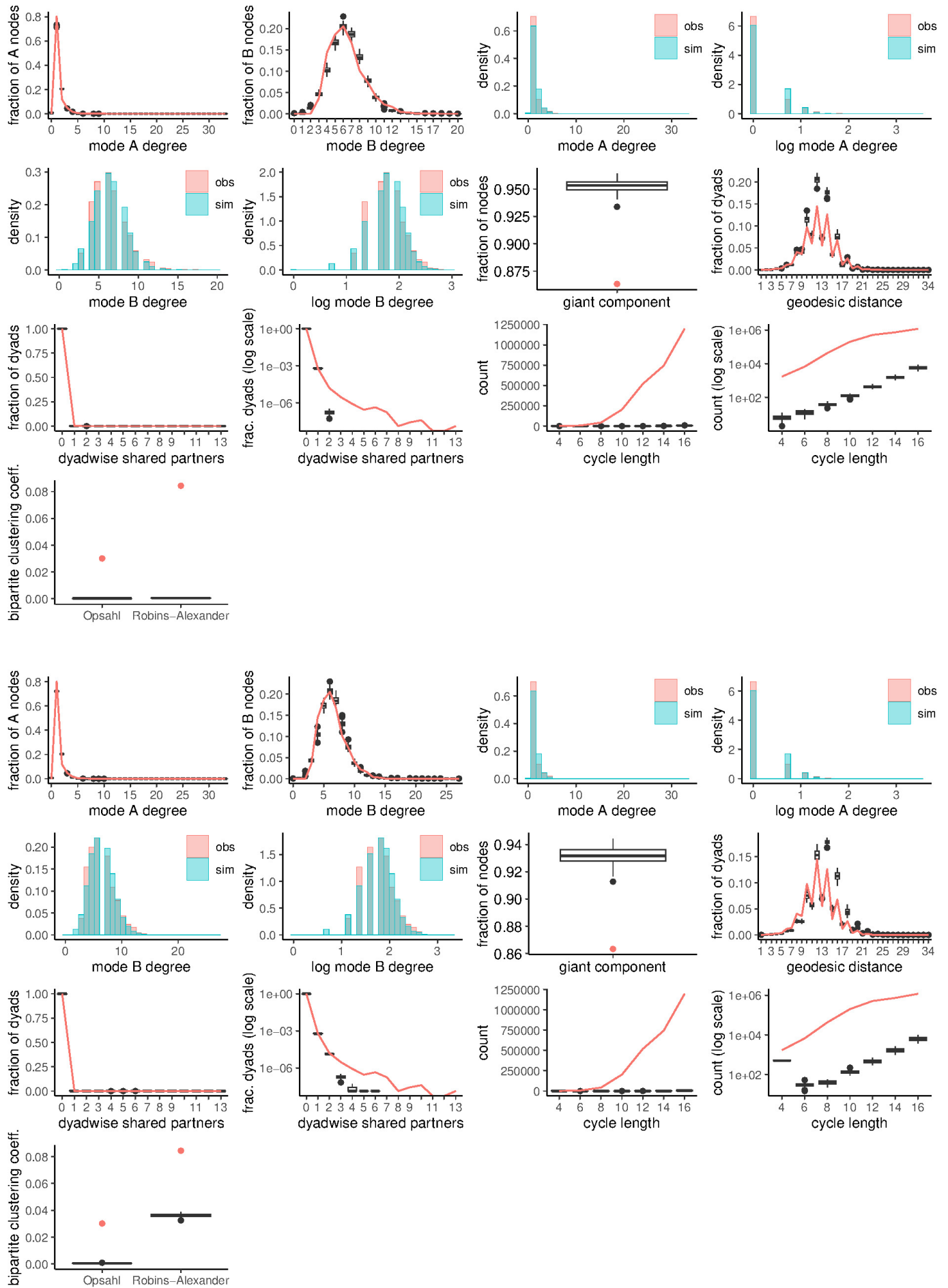


Figure D4: Goodness-of-fit plots for the Australian director interlock network ERGM (Table 8) Model 2 (top) and Model 3 (bottom). The observed network statistics are plotted in red with the statistics of 100 simulated networks plotted as black box plots, and blue on the histograms.

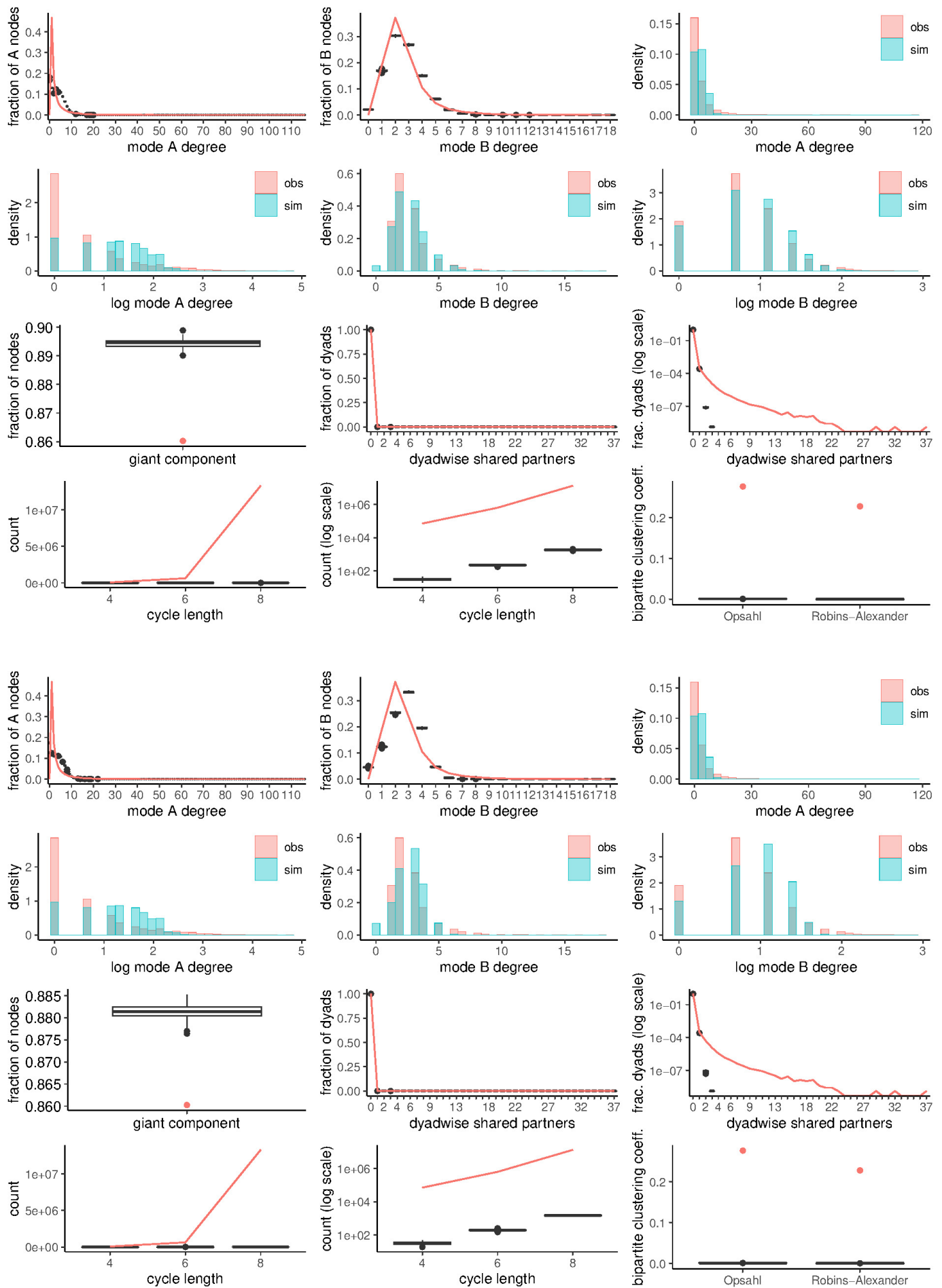


Figure D5: Goodness-of-fit plots for the scientific collaboration network ERGM (Table 9) Model 1 (top) and Model 2 (bottom). The observed network statistics are plotted in red with the statistics of 100 simulated networks plotted as black box plots, and blue on the histograms.

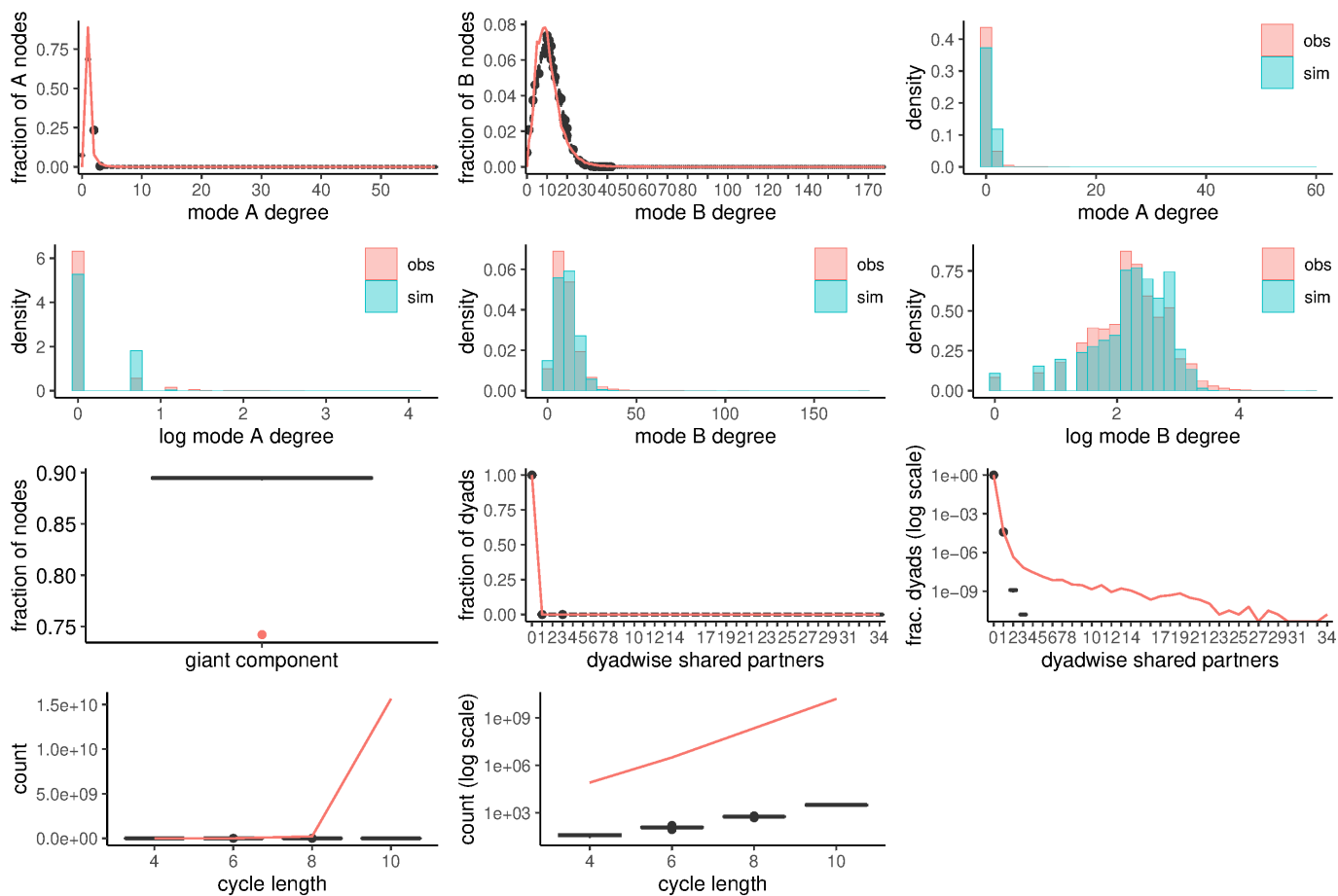


Figure D6: Goodness-of-fit plots for the international director interlock network ERGM (Table 10) Model 3. The observed network statistics are plotted in red with the statistics of 100 simulated networks plotted as black box plots, and blue on the histograms.

E Supplementary Tables

Table E1: Four-cycle descriptive statistics.

Network	N_A	N_B	4-cycles	Unique nodes in 4-cycles	
				A	B
Inouye-Pyke pollinators	91	42	830	47	33
St Louis crime	870	557	144	93	121
Norwegian director interlock	1 495	367	108	89	77
Robertson pollinators	1 428	456	565 969	862	456
Australian director interlock	9 971	2 087	1 743	742	663
Scientific collaborations	16 726	22 015	70 549	7 604	14 137
International director interlock	321 869	34 769	79 885	12 567	8 136

Table E2: ERGM parameter estimates from MPNet for the Inouye-Pyke pollinator web. * indicates statistical significance at the nominal 95% level.

Effects	Lambda	Parameter	Stderr	t-ratio	
XEdge	2.0000	-5.5726	0.197	0.024	*
XASA	2.0000	0.7998	0.127	0.022	*
XASB	2.0000	0.7301	0.174	0.020	*
XACB	2.0000	0.0730	0.002	-0.012	*

References

- [1] Ronald L Breiger. The duality of persons and groups. *Soc Forces*, 53(2):181–190, 1974.
- [2] Zachary P. Neal, Annabell Cadieux, Diego Garlaschelli, Nicholas J. Gotelli, Fabio Saracco, Tiziano Squartini, Shade T. Shuttters, Werner Ulrich, Guanyang Wang, and Giovanni Strona. Pattern detection in bipartite networks: A review of terminology, applications, and methods. *PLOS Complex Syst*, 1(2):e0000010, 10 2024.
- [3] Peng Wang, Garry Robins, Philippa Pattison, and Emmanuel Lazega. Exponential random graph models for multilevel networks. *Soc Netw*, 35(1):96–115, 2013.
- [4] Matthieu Latapy, Clémence Magnien, and Nathalie Del Vecchio. Basic notions for the analysis of large two-mode networks. *Soc Netw*, 30(1):31–48, 2008.
- [5] Martin G Everett and Stephen P Borgatti. The dual-projection approach for two-mode networks. *Soc Netw*, 35(2):204–210, 2013.
- [6] Martin G Everett. Centrality and the dual-projection approach for two-mode social network data. *Method Innov*, 9:2059799116630662, 2016.
- [7] Mark S. Granovetter. The strength of weak ties. *Am J Sociol*, 78(6):1360–1380, 1973.
- [8] Eric W. Weisstein. Bipartite graph. From MathWorld—A Wolfram Web Resource. <https://mathworld.wolfram.com/BipartiteGraph.html>, 2024.
- [9] Garry Robins and Malcolm Alexander. Small worlds among interlocking directors: Network structure and distance in bipartite graphs. *Comput Math Organ Theory*, 10(1):69–94, 2004.
- [10] Tore Opsahl. Triadic closure in two-mode networks: Redefining the global and local clustering coefficients. *Soc Netw*, 35(2):159–167, 2013.

- [11] Dean Lusher, Johan Koskinen, and Garry Robins, editors. *Exponential Random Graph Models for Social Networks: Theory, Methods, and Applications*. Structural Analysis in the Social Sciences. Cambridge University Press, New York, 2013.
- [12] Viviana Amati, Alessandro Lomi, and Antonietta Mira. Social network modeling. *Annu Rev Stat Appl*, 5:343–369, 2018.
- [13] J. Koskinen. Exponential random graph modelling. In P. Atkinson, S. Delamont, A. Cernat, J.W. Sakshaug, and R.A. Williams, editors, *SAGE Research Methods Foundations*. SAGE, London, 2020. <https://doi.org/10.4135/9781526421036888175>.
- [14] Johan Koskinen. Exponential random graph models. In John McLevey, John Scott, and Peter J Carrington, editors, *The Sage Handbook of Social Network Analysis*, chapter 33. Sage, second edition, 2023.
- [15] Giulio Cimini, Tiziano Squartini, Fabio Saracco, Diego Garlaschelli, Andrea Gabrielli, and Guido Caldarelli. The statistical physics of real-world networks. *Nat Rev Phys*, 1(1):58–71, 2019.
- [16] Saeid Ghafouri and Seyed Hossein Khasteh. A survey on exponential random graph models: an application perspective. *PeerJ Comput Sci*, 6:e269, 2020.
- [17] Francesco Giacomarra, Gianmarco Bet, and Alessandro Zocca. Generating synthetic power grids using exponential random graph models. *PRX Energy*, 3(2):023005, 2024.
- [18] Peng Wang, Ken Sharpe, Garry L Robins, and Philippa E Pattison. Exponential random graph (p^*) models for affiliation networks. *Soc Netw*, 31(1):12–25, 2009.
- [19] Peng Wang, Philippa Pattison, and Garry Robins. Exponential random graph model specifications for bipartite networks—a dependence hierarchy. *Soc Netw*, 35(2):211–222, 2013.
- [20] Peng Wang. Exponential random graph model extensions: Models for multiple networks and bipartite networks. In Dean Lusher, Johan Koskinen, and Garry Robins, editors, *Exponential Random Graph Models for Social Networks: Theory, Methods, and Applications*, chapter 10, pages 115–129. Cambridge University Press, New York, 2013.
- [21] Rashmi P Bomiriya, Alina R Kuvelkar, David R Hunter, and Steffen Triebel. Modeling homophily in exponential-family random graph models for bipartite networks. *arXiv preprint arXiv:2312.05673v1*, 2023.
- [22] Philippa E. Pattison and T.A.B. Snijders. Modeling social networks: Next steps. In Dean Lusher, Johan Koskinen, and Garry Robins, editors, *Exponential Random Graph Models for Social Networks: Theory, Methods, and Applications*, chapter 22, pages 287–301. Cambridge University Press, New York, 2013.
- [23] Charles J Geyer and Elizabeth A Thompson. Constrained Monte Carlo maximum likelihood for dependent data. *J R Stat Soc B*, 54(3):657–683, 1992.
- [24] Tom A. B. Snijders. Markov chain Monte Carlo estimation of exponential random graph models. *J Soc Struct*, 3(2):1–40, 2002.
- [25] David R Hunter, Pavel N Krivitsky, and Michael Schweinberger. Computational statistical methods for social network models. *J Comput Graph Stat*, 21(4):856–882, 2012.
- [26] Maksym Byshkin, Alex Stivala, Antonietta Mira, Rolf Krause, Garry Robins, and Alessandro Lomi. Auxiliary parameter MCMC for exponential random graph models. *J Stat Phys*, 165(4):740–754, 2016.
- [27] Maksym Byshkin, Alex Stivala, Antonietta Mira, Garry Robins, and Alessandro Lomi. Fast maximum likelihood estimation via equilibrium expectation for large network data. *Sci Rep*, 8(1):11509, 2018.
- [28] Alexander Borisenko, Maksym Byshkin, and Alessandro Lomi. A simple algorithm for scalable Monte Carlo inference. *arXiv preprint arXiv:1901.00533v4*, 2020.

- [29] Mark S Handcock. Assessing degeneracy in statistical models of social networks. Working Paper no. 39, Center for Statistics and the Social Sciences, University of Washington, 2003. <https://csss.uw.edu/Papers/wp39.pdf>.
- [30] Tom A. B. Snijders, Philippa E. Pattison, Garry L. Robins, and Mark S. Handcock. New specifications for exponential random graph models. *Sociol Methodol*, 36(1):99–153, 2006.
- [31] Ian Fellows and Mark Handcock. Removing phase transitions from Gibbs measures. In Aarti Singh and Jerry Zhu, editors, *Proceedings of the 20th International Conference on Artificial Intelligence and Statistics*, volume 54 of *Proceedings of Machine Learning Research*, pages 289–297, 20–22 Apr 2017.
- [32] Michael Schweinberger. Instability, sensitivity, and degeneracy of discrete exponential families. *J Am Stat Assoc*, 106(496):1361–1370, 2011.
- [33] Sourav Chatterjee and Persi Diaconis. Estimating and understanding exponential random graph models. *Ann Stat*, 41(5):2428–2461, 2013.
- [34] Michael Schweinberger. Consistent structure estimation of exponential-family random graph models with block structure. *Bernoulli*, 26(2):1205–1233, 2020.
- [35] Bart Blackburn and Mark S Handcock. Practical network modeling via tapered exponential-family random graph models. *J Comput Graph Stat*, 32(2):388–401, 2023.
- [36] Garry Robins, Tom A. B. Snijders, Peng Wang, Mark Handcock, and Philippa Pattison. Recent developments in exponential random graph (p^*) models for social networks. *Soc Netw*, 29(2):192–215, 2007.
- [37] J. Koskinen and G. Daraganova. Exponential random graph model fundamentals. In Dean Lusher, Johan Koskinen, and Garry Robins, editors, *Exponential Random Graph Models for Social Networks: Theory, Methods, and Applications*, chapter 6, pages 49–76. Cambridge University Press, New York, 2013.
- [38] David R. Hunter. Curved exponential family models for social networks. *Soc Netw*, 29(2):216–230, 2007.
- [39] Alex Stivala. Overcoming near-degeneracy in the autologistic actor attribute model. *arXiv preprint arXiv:2309.07338v2*, 2023.
- [40] David R. Hunter and Mark S. Handcock. Inference in curved exponential family models for networks. *J Comput Graph Stat*, 15(3):565–583, 2006.
- [41] Mark S. Handcock, David R. Hunter, Carter T. Butts, Steven M. Goodreau, and Martina Morris. statnet: Software tools for the representation, visualization, analysis and simulation of network data. *J Stat Softw*, 24(1):1–11, 2008.
- [42] Mark S. Handcock, David R. Hunter, Carter T. Butts, Steven M. Goodreau, Pavel N. Krivitsky, Skye Bender-deMoll, and Martina Morris. *statnet: Software Tools for the Statistical Analysis of Network Data*. The Statnet Project (<http://www.statnet.org>), 2016. R package version 2019.6. <https://CRAN.R-project.org/package=statnet>.
- [43] P. Wang, G. Robins, and P. Pattison. *PNet: program for the estimation and simulation of p^* exponential random graph models*. Department of Psychology, The University of Melbourne, 2009. <https://www.melnet.org.au/s/PNetManual.pdf>.
- [44] Peng Wang, Garry Robins, Philippa Pattison, and JH Koskinen. *MPNet: Program for the simulation and estimation of (p^*) exponential random graph models for multilevel networks*. Melbourne School of Psychological Sciences, The University of Melbourne, 2014. <http://www.melnet.org.au/s/MPNetManual.pdf>.
- [45] Peng Wang, Alex Stivala, Garry Robins, Philippa Pattison, Johan Koskinen, and Alessandro Lomi. *PNet: Program for the simulation and estimation of (p^*) exponential random graph models for multilevel networks*, 2022. <http://www.melnet.org.au/s/MPNetManual2022.pdf>.

- [46] David R Hunter, Mark S Handcock, Carter T Butts, Steven M Goodreau, and Martina Morris. *ergm*: A package to fit, simulate and diagnose exponential-family models for networks. *J Stat Softw*, 24(3):1–29, 2008.
- [47] Ruth M. Hummel, David R. Hunter, and Mark S. Handcock. Improving simulation-based algorithms for fitting ERGMs. *J Comput Graph Stat*, 21(4):920–939, 2012.
- [48] Mark S. Handcock, David R. Hunter, Carter T. Butts, Steven M. Goodreau, Pavel N. Krivitsky, and Martina Morris. *ergm: Fit, Simulate and Diagnose Exponential-Family Models for Networks*. The Statnet Project (<https://statnet.org>), 2024. R package version 4.7.5. <https://CRAN.R-project.org/package=ergm>.
- [49] Pavel N. Krivitsky, David R. Hunter, Martina Morris, and Chad Klumb. *ergm* 4: New features for analyzing exponential-family random graph models. *J Stat Softw*, 105(6):1–44, 2023.
- [50] Pavel N Krivitsky, David R Hunter, Martina Morris, and Chad Klumb. *ergm* 4: Computational improvements. *arXiv preprint arXiv:2203.08198v1*, 2022.
- [51] Alberto Caimo and Nial Friel. *Bergm*: Bayesian exponential random graphs in R. *J Stat Softw*, 61(2):1–25, 2014.
- [52] Alberto Caimo, Lampros Bouranis, Robert Krause, and Nial Friel. Statistical network analysis with *Bergm*. *J Stat Softw*, 104(1):1–23, 2022.
- [53] Jessica Balest, Laura Secco, Elena Pisani, and Alberto Caimo. Sustainable energy governance in South Tyrol (Italy): A probabilistic bipartite network model. *J Clean Prod*, 221:854–862, 2019.
- [54] Filip Agneessens and Henk Roose. Local structural properties and attribute characteristics in 2-mode networks: p^* models to map choices of theater events. *J Math Sociol*, 32(3):204–237, 2008.
- [55] Richard A. Benton and Jihae You. Endogenous dynamics in contentious fields: Evidence from the shareholder activism network, 2006–2013. *Socius*, 3:2378023117705231, 2017.
- [56] Mark Lubell and Matthew Robbins. Adapting to sea-level rise: Centralization or decentralization in polycentric governance systems? *Policy Stud J*, 50(1):143–175, 2022.
- [57] Duncan J. Watts and Steven H. Strogatz. Collective dynamics of ‘small-world’ networks. *Nature*, 393(6684):440–442, 1998.
- [58] Mark EJ Newman and Juyong Park. Why social networks are different from other types of networks. *Phys Rev E*, 68(3):036122, 2003.
- [59] Duncan A Clark and Mark S Handcock. Comparing the real-world performance of exponential-family random graph models and latent order logistic models for social network analysis. *J R Stat Soc A*, 185(2):566–587, 2022.
- [60] Ian E Fellows. A new generative statistical model for graphs: The latent order logistic (LOLOG) model. *arXiv preprint arXiv:1804.04583v1*, 2018.
- [61] Birgit Pauksztat, Christian Steglich, and Rafael Wittek. Who speaks up to whom? a relational approach to employee voice. *Soc Netw*, 33(4):303–316, 2011.
- [62] Patrick Doreian and Norman Conti. Social context, spatial structure and social network structure. *Soc Netw*, 34(1):32–46, 2012. Capturing Context: Integrating Spatial and Social Network Analyses.
- [63] Ling Heng Henry Wong, André F. Gygax, and Peng Wang. Board interlocking network and the design of executive compensation packages. *Soc Netw*, 41:85–100, 2015.
- [64] Steven M. Goodreau. Advances in exponential random graph (p^*) models applied to a large social network. *Soc Netw*, 29(2):231–248, 2007.

- [65] Richard Heidler, Markus Gamper, Andreas Herz, and Florian Eßer. Relationship patterns in the 19th century: The friendship network in a German boys' school class from 1880 to 1881 revisited. *Soc Netw*, 37:1–13, 2014.
- [66] Kerstin Sailer and Ian McCulloh. Social networks and spatial configuration—how office layouts drive social interaction. *Soc Netw*, 34(1):47–58, 2012. Capturing Context: Integrating Spatial and Social Network Analyses.
- [67] Manuel Fischer and Pascal Sciarini. Unpacking reputational power: Intended and unintended determinants of the assessment of actors' power. *Soc Netw*, 42:60–71, 2015.
- [68] Riitta Toivonen, Lauri Kovanen, Mikko Kivelä, Jukka-Pekka Onnela, Jari Saramäki, and Kimmo Kaski. A comparative study of social network models: Network evolution models and nodal attribute models. *Soc Netw*, 31(4):240–254, 2009.
- [69] Robert Ackland and Mathieu O'Neil. Online collective identity: The case of the environmental movement. *Soc Netw*, 33(3):177–190, 2011.
- [70] Carolyn J Anderson, Stanley Wasserman, and Bradley Crouch. A p* primer: logit models for social networks. *Soc Netw*, 21(1):37–66, 1999.
- [71] Alex Stivala, Garry Robins, and Alessandro Lomi. Exponential random graph model parameter estimation for very large directed networks. *PLoS One*, 15(1):e0227804, 2020.
- [72] Nicholas Harrigan and Matthew Bond. Differential impact of directors' social and financial capital on corporate interlock formation. In Dean Lusher, Johan Koskinen, and Garry Robins, editors, *Exponential Random Graph Models for Social Networks: Theory, Methods, and Applications*, chapter 20, pages 260–271. Cambridge University Press, New York, 2013.
- [73] Alex Stivala. Geodesic cycle length distributions in delusional and other social networks. *J Soc Struct*, 21(1):35–76, 2020.
- [74] Alex Stivala. Geodesic cycle length distributions in fictional character networks. *arXiv preprint arXiv:2303.11597v1*, 2023.
- [75] John Levi Martin. Comment on geodesic cycle length distributions in delusional and other social networks. *J Soc Struct*, 21(1):77–93, 2020.
- [76] James D Wilson, Matthew J Denny, Shankar Bhamidi, Skyler J Cranmer, and Bruce A Desmarais. Stochastic weighted graphs: Flexible model specification and simulation. *Soc Netw*, 49:37–47, 2017.
- [77] Philippa E. Pattison, Garry L. Robins, Tom A.B. Snijders, and Peng Wang. Exponential random graph models and pendant-triangle statistics. *Soc Netw*, 79:187–197, 2024.
- [78] Philippa Pattison and Garry Robins. Neighborhood-based models for social networks. *Sociol Methodol*, 32(1):301–337, 2002.
- [79] Philippa Pattison and Garry Robins. Building models for social space: Neighbourhood-based models for social networks and affiliation structures. *Math & Sci Hum*, 42(168):11–29, 2004.
- [80] David R. Hunter, Steven M. Goodreau, and Mark S. Handcock. `ergm.userterms`: A template package for extending `statnet`. *J Stat Softw*, 52(2):1–25, 2013.
- [81] David R Hunter and Steven M Goodreau. Extending ERGM functionality within `statnet`: Building custom user terms. https://statnet.org/workshop-ergm-userterms/ergm.userterms_tutorial.pdf, 2019. Statnet Development Team.
- [82] Takeaki Uno and Hiroko Satoh. An efficient algorithm for enumerating chordless cycles and chordless paths. In Sašo Džeroski, Panče Panov, Dragi Kocev, and Ljupčo Todorovski, editors, *International Conference on Discovery Science*, volume 8777 of *LNAI*, pages 313–324. Springer, 2014.

- [83] R Core Team. *R: A Language and Environment for Statistical Computing*. R Foundation for Statistical Computing, Vienna, Austria, 2022.
- [84] Gábor Csárdi and Tamas Nepusz. The igraph software package for complex network research. *InterJournal, Complex Systems*:1695, 2006.
- [85] Michael Antonov, Gábor Csárdi, Szabolcs Horvát, Kirill Müller, Tamás Nepusz, Daniel Noom, Maëlle Salmon, Vincent Traag, Brooke Foucault Welles, and Fabio Zanini. igraph enables fast and robust network analysis across programming languages. *arXiv preprint arXiv:2311.10260v1*, 2023.
- [86] Hadley Wickham. *ggplot2: Elegant Graphics for Data Analysis*. Springer-Verlag, New York, 2016.
- [87] Martina Morris, Mark Handcock, and David Hunter. Specification of exponential-family random graph models: Terms and computational aspects. *J Stat Softw*, 24(4):1–24, 2008.
- [88] Mark S Mizruchi. What do interlocks do? an analysis, critique, and assessment of research on interlocking directorates. *Annu Rev Sociol*, 22(1):271–298, 1996.
- [89] David W Inouye and Graham H Pyke. Pollination biology in the Snowy Mountains of Australia: comparisons with montane Colorado, USA. *Aust J Ecol*, 13(2):191–205, 1988.
- [90] Alex Stivala and Alessandro Lomi. A new scalable implementation of the citation exponential random graph model (cERGM) and its application to a large patent citation network. Talk presented at INSNA Sunbelt XLII conference, July 2022. <https://doi.org/10.5281/zenodo.7951927>.
- [91] Alex Stivala, Peng Wang, and Alessandro Lomi. ALAAMEE: Open-source software for fitting autologistic actor attribute models. *PLOS Complex Syst*, 1(4):e0000021, 2024.
- [92] S. Decker, C. W. Kohfeld, R. Rosenfeld, and J. Sprague. *The St. Louis Homicide Project: Local Responses to a National Problem*. University of Missouri–St. Louis, 1991.
- [93] David Schoch. networkdata: Repository of network datasets, October 2022. <https://doi.org/10.5281/zenodo.7189928>.
- [94] Charles Robertson. *Flowers and insects; lists of visitors of four hundred and fifty-three flowers*. Science Press Printing Company, Lancaster, Pennsylvania, USA, 1928.
- [95] John C. Marlin and Wallace E. LaBerge. The native bee fauna of Carlinville, Illinois, revisited after 75 years: a case for persistence. *Conserv Ecol*, 5(1), 2001.
- [96] Alex Stivala and Alessandro Lomi. Testing biological network motif significance with exponential random graph models. *Appl Netw Sci*, 6(1):91, 2021.
- [97] Alex Stivala. New network models facilitate analysis of biological networks. *arXiv preprint arXiv:2312.06047v1*, 2023.
- [98] Mark S. Handcock, Pavel N. Krivitsky, and Ian Fellows. *ergm.tapered: Tapered Exponential-Family Models for Networks*, 2022. R package version 1.1-0. <https://github.com/statnet/ergm.tapered>.
- [99] Cathrine Seierstad and Tore Opsahl. For the few not the many? the effects of affirmative action on presence, prominence, and social capital of women directors in Norway. *Scand J Manag*, 27(1):44–54, 2011.
- [100] A. Stivala, P. Wang, and A. Lomi. Numbers and structural positions of women in a national director interlock network. Talk presented at INSNA Sunbelt XLIII Conference, June 2023. <https://doi.org/10.5281/zenodo.8092829>.
- [101] Mark E. J. Newman. The structure of scientific collaboration networks. *Proc Natl Acad Sci USA*, 98(2):404–409, 2001.
- [102] Mark E. J. Newman. Scientific collaboration networks. I. Network construction and fundamental results. *Phys Rev E*, 64(1):016131, 2001.

- [103] Mark E. J. Newman. Scientific collaboration networks. II. Shortest paths, weighted networks, and centrality. *Phys Rev E*, 64(1):016132, 2001.
- [104] Anna Evtushenko and Michael T. Gastner. Beyond Fortune 500: Women in a global network of directors. In Hocine Cherifi, Sabrina Gaito, José Fernando Mendes, Esteban Moro, and Luis Mateus Rocha, editors, *Complex Networks and Their Applications VIII*, pages 586–598, Cham, 2020. Springer International Publishing.
- [105] Anna Evtushenko and Michael T. Gastner. Data set discussed in “Beyond Fortune 500: Women in a Global Network of Directors”, November 2019. <https://doi.org/10.5281/zenodo.3553442>.
- [106] Michael Levy, Mark Lubell, Philip Leifeld, and Skyler Cranmer. Interpretation of gw-degree estimates in ERGMs, June 2016. <https://doi.org/10.6084/m9.figshare.3465020.v1>.
- [107] Michael Levy. gwdegree: Improving interpretation of geometrically-weighted degree estimates in exponential random graph models. *J Open Source Softw*, 1(3):36, 2016.
- [108] Alex Stivala. Reply to “Comment on geodesic cycle length distributions in delusional and other social networks”. *J Soc Struct*, 21(1):94–106, 2020.
- [109] Ian E. Fellows. *lolog: Latent Order Logistic Graph Models*, 2023. R package version 1.3.1. <https://CRAN.R-project.org/package=lolog>.
- [110] Filip Agneessens, Henk Roose, and Hans Waege. Choices of theatre events: p* models for affiliation networks with attributes. *Metod Zv*, 1(2):419–439, 2004.
- [111] Ramiro Berardo. Bridging and bonding capital in two-mode collaboration networks. *Policy Stud J*, 42(2):197–225, 2014.
- [112] Youyi Bi, Yunjian Qiu, Zhenghui Sha, Mingxian Wang, Yan Fu, Noshir Contractor, and Wei Chen. Modeling multi-year customers’ considerations and choices in China’s auto market using two-stage bipartite network analysis. *Netw Spat Econ*, 21(2):365–385, 2021.
- [113] Matthew Bond. The bases of elite social behaviour: Patterns of club affiliation among members of the House of Lords. *Sociology*, 46(4):613–632, 2012.
- [114] Laurence Brandenberger, Isabelle Schläpfer, Philip Leifeld, and Manuel Fischer. Interrelated issues and overlapping policy sectors: Swiss water politics. <http://nbn-resolving.de/urn:nbn:de:bsz:352-0-294740>, 2015.
- [115] Guido Conaldi and Alessandro Lomi. The dual network structure of organizational problem solving: A case study on open source software development. *Soc Netw*, 35(2):237–250, 2013.
- [116] Camille DeSisto and James Paul Herrera. Drivers and consequences of structure in plant–lemur ecological networks. *J Anim Ecol*, 91(10):2010–2022, 2022.
- [117] Scott W. Duxbury and Dana L. Haynie. Building them up, breaking them down: Topology, vendor selection patterns, and a digital drug market’s robustness to disruption. *Soc Netw*, 52:238–250, 2018.
- [118] Scott W Duxbury and Dana L Haynie. The network structure of opioid distribution on a darknet cryptomarket. *J Quant Criminol*, 34(4):921–941, 2018.
- [119] Katherine Faust, Karin E Willert, David D Rowlee, and John Skvoretz. Scaling and statistical models for affiliation networks: patterns of participation among Soviet politicians during the Brezhnev era. *Soc Netw*, 24(3):231–259, 2002.
- [120] Harrison S Fried, Matthew Hamilton, and Ramiro Berardo. Closing integrative gaps in complex environmental governance systems. *Ecol Soc*, 27(1):15, 2022.
- [121] Cornelius Fritz, Giacomo De Nicola, Sevag Kevork, Dietmar Harhoff, and Göran Kauermann. Modelling the large and dynamically growing bipartite network of German patents and inventors. *J R Stat Soc Ser A Stat Soc*, 186(3):557–576, 03 2023.

- [122] Lisieux Fuzessy, Gisela Sobral, Daiane Carreira, Débora Cristina Rother, Gedimar Barbosa, Mariana Landis, Mauro Galetti, Tad Dallas, Vinícius Cardoso Cláudio, Laurence Culot, and Pedro Jordano. Functional roles of frugivores and plants shape hyper-diverse mutualistic interactions under two antagonistic conservation scenarios. *Biotropica*, 54(2):444–454, 2022.
- [123] Caleb Gallemore, Monica Di Gregorio, Moira Moeliono, Maria Brockhaus, and Rut Dini Prasti H. Transaction costs, power, and multi-level forest governance in Indonesia. *Ecol Econ*, 114:168–179, 2015.
- [124] Neha Gondal. The local and global structure of knowledge production in an emergent research field: An exponential random graph analysis. *Soc Netw*, 33(1):20–30, 2011.
- [125] Neha Gondal. Duality of departmental specializations and PhD exchange: A Weberian analysis of status in interaction using multilevel exponential random graph models (mERGM). *Soc Netw*, 55:202–212, 2018.
- [126] Matthew Hamilton, Mark Lubell, and Emilinah Namaganda. Cross-level linkages in an ecology of climate change adaptation policy games. *Ecol Soc*, 23(2):36, 2018.
- [127] Cilem Hazir and Corinne Autant-Bernard. Using affiliation networks to study the determinants of multilateral research cooperation: some empirical evidence from eu framework programs in biotechnology. Working Paper 1212, GATE, 2012. <https://doi.org/10.2139/ssrn.2060275>.
- [128] Michael T. Heaney and Philip Leifeld. Contributions by interest groups to lobbying coalitions. *J Polit*, 80(2):494–509, 2018.
- [129] Yun Huang, Mengxiao Zhu, Jing Wang, Nishith Pathak, Cuihua Shen, Brian Keegan, Dmitri Williams, and Noshir Contractor. The formation of task-oriented groups: Exploring combat activities in online games. In *2009 International Conference on Computational Science and Engineering*, volume 4, pages 122–127, 2009.
- [130] Lorien Jasny. Baseline models for two-mode social network data. *Policy Stud J*, 40(3):458–491, 2012.
- [131] Lorien Jasny and Mark Lubell. Two-mode brokerage in policy networks. *Soc Netw*, 41:36–47, 2015.
- [132] Brian Keegan, Darren Gergle, and Noshir Contractor. Do editors or articles drive collaboration? multilevel statistical network analysis of Wikipedia coauthorship. In *Proceedings of the ACM 2012 Conference on Computer Supported Cooperative Work, CSCW '12*, page 427–436, New York, NY, USA, 2012. Association for Computing Machinery.
- [133] Sevag Kevork and Göran Kauermann. Bipartite exponential random graph models with nodal random effects. *Soc Netw*, 70:90–99, 2022.
- [134] Jalayer Khalilzadeh. Demonstration of exponential random graph models in tourism studies: Is tourism a means of global peace or the bottom line? *Ann Tour Res*, 69:31–41, 2018.
- [135] Chih-Hui Lai, Chen-Chao Tao, and Yu-Chung Cheng. Modeling resource network relationships between response organizations and affected neighborhoods after a technological disaster. *Voluntas*, 28(5):2145–2175, 2017.
- [136] Philip Leifeld and Thomas Malang. National parliamentary coordination after Lisbon: A network approach. Paper prepared for the 1st European Conference on Social Networks (EUSN), Barcelona, Spain, July 2014.
- [137] Qingchun Li and Ali Mostafavi. Local interactions and homophily effects in actor collaboration networks for urban resilience governance. *Appl Netw Sci*, 6(1):89, 2021.
- [138] Yingjie Lu and Qian Wang. Doctors’ preferences in the selection of patients in online medical consultations: an empirical study with doctor–patient consultation data. *Healthcare*, 10(8):1435, 2022.
- [139] Mark Lubell, Garry Robins, and Peng Wang. Network structure and institutional complexity in an ecology of water management games. *Ecol Soc*, 19(4):23, 2014.

- [140] Drew Margolin, K Ognyanoya, Meikuan Huang, Yun Huang, and Noshir Contractor. Team formation and performance on nanoHub: a network selection challenge in scientific communities. In Balázs Vedres and Marco Scotti, editors, *Networks in Social Policy Problems*, chapter 5, page 80–100. Cambridge University Press, 2012.
- [141] Rebecca L Mauldin, Carin Wong, Jason Fernandez, and Kayo Fujimoto. Network modeling of assisted living facility residents’ attendance at programmed group activities: Proximity and social contextual correlates of attendance. *Gerontologist*, 61(5):703–713, 2021.
- [142] Ryan RJ McAllister, Rod McCrea, and Mark N Lubell. Policy networks, stakeholder interactions and climate adaptation in the region of South East Queensland, Australia. *Reg Environ Change*, 14(2):527–539, 2014.
- [143] Ryan RJ McAllister, Catherine J Robinson, Kirsten Maclean, Angela M Guerrero, Kerry Collins, Bruce M Taylor, and Paul J De Barro. From local to central: a network analysis of who manages plant pest and disease outbreaks across scales. *Ecol Soc*, 20(1):67, 2015.
- [144] Ryan RJ McAllister, Bruce M Taylor, and Ben P Harman. Partnership networks for urban development: how structure is shaped by risk. *Policy Stud J*, 43(3):379–398, 2015.
- [145] Ryan RJ McAllister, Catherine J Robinson, Alinta Brown, Kirsten Maclean, Suzy Perry, and Shuang Liu. Balancing collaboration with coordination: contesting eradication in the Australian plant pest and disease biosecurity system. *Int J Commons*, 11(1):330–354, 2017.
- [146] Florence Metz, Philip Leifeld, and Karin Ingold. Interdependent policy instrument preferences: a two-mode network approach. *J Public Policy*, 39(4):609–636, 2019.
- [147] Anne-Marie Niekamp, Liesbeth AG Mercken, Christian JPA Hoebe, and Nicole HTM Dukers-Muijers. A sexual affiliation network of swingers, heterosexuals practicing risk behaviours that potentiate the spread of sexually transmitted infections: a two-mode approach. *Soc Netw*, 35(2):223–236, 2013.
- [148] Andreea Nita, Laurentiu Rozyłowicz, Steluta Manolache, Cristiana Maria Ciocănea, Iulia Viorica Miu, and Viorel Dan Popescu. Collaboration networks in applied conservation projects across Europe. *PLoS One*, 11(10):e0164503, 2016.
- [149] Lukas Norbutas. Offline constraints in online drug marketplaces: An exploratory analysis of a cryptomarket trade network. *Int J Drug Policy*, 56:92–100, 2018.
- [150] Sejung Park and Rong Wang. Assessing the capability of government information intervention and socioeconomic factors of information sharing during the COVID-19 pandemic: a cross-country study using big data analytics. *Behav Sci*, 12(6):190, 2022.
- [151] Hang Ren, Lu Zhang, Travis A Whetsell, and N Emel Ganapati. Analyzing multisector stakeholder collaboration and engagement in housing resilience planning in greater Miami and the beaches through social network analysis. *Nat Hazards Rev*, 24(1):04022036, 2023.
- [152] Juan Carlos Rocha, Garry D Peterson, and ReINETTE Biggs. Regime shifts in the Anthropocene: drivers, risks, and resilience. *PLoS One*, 10(8):e0134639, 2015.
- [153] Tyler A Scott and Craig W Thomas. Winners and losers in the ecology of games: Network position, connectivity, and the benefits of collaborative governance regimes. *J Public Adm Res Theory*, 27(4):647–660, 2017.
- [154] Zhenghui Sha, Youyi Bi, Mingxian Wang, Amanda Stathopoulos, Noshir Contractor, Yan Fu, and Wei Chen. Comparing utility-based and network-based approaches in modeling customer preferences for engineering design. In *Proceedings of the Design Society: International Conference on Engineering Design*, volume 1, pages 3831–3840, 2019.
- [155] Zhenghui Sha, Ashish M Chaudhari, and Jitesh H Panchal. Modeling participation behaviors in design crowdsourcing using a bipartite network-based approach. *J Comput Inf Sci Eng*, 19(3):031010, 2019.

- [156] Seongmin Shin, Mi Sun Park, Hansol Lee, and Himlal Baral. The structure and pattern of global partnerships in the REDD+ mechanism. *For Policy Econ*, 135:102640, 2022.
- [157] John A Shjarback and Jacob TN Young. The “tough on crime” competition: A network approach to understanding the social mechanisms leading to federal crime control legislation in the United States from 1973–2014. *Am, J Crim Just*, 43(2):197–221, 2018.
- [158] Bryan Stephens, Wenhong Chen, and John Sibley Butler. Bubbling up the good ideas: A two-mode network analysis of an intra-organizational idea challenge. *J Comput Mediat Commun*, 21(3):210–229, 2016.
- [159] Rong Wang. Marginality and team building in collaborative crowdsourcing. *Online Inf Rev*, 44(4):827–846, 2020.
- [160] Arndt Wonka and Sebastian Haunss. Cooperation in networks: political parties and interest groups in EU policy-making in Germany. *Eur Union Polit*, 21(1):130–151, 2020.
- [161] Mengxiao Zhu, Yun Huang, and Noshir S Contractor. Motivations for self-assembling into project teams. *Soc Netw*, 35(2):251–264, 2013.
- [162] Allison Davis, Burleigh B Gardner, Mary R Gardner, and W Lloyd Warner. *Deep South: A sociological anthropological study of caste and class*. University of Chicago Press, 1941.
- [163] Pavel N. Krivitsky and Mark S. Handcock. Fitting position latent cluster models for social networks with latentnet. *J Stat Softw*, 24(5), 2008.
- [164] Pavel N. Krivitsky and Mark S. Handcock. *latentnet: Latent Position and Cluster Models for Statistical Networks*. The Statnet Project (<https://statnet.org>), 2024. R package version 2.11.0. <https://CRAN.R-project.org/package=latentnet>.
- [165] Philip Leifeld. texreg: Conversion of statistical model output in R to L^AT_EX and HTML tables. *J Stat Softw*, 55(8):1–24, 2013.